

A SMALL PERTURBATION THEORY
FOR CYCLOIDAL PROPELLERS

Thesis by
Edwin C. James

In Partial Fulfillment of the Requirements for
the Degree of Doctor of Philosophy

California Institute of Technology
Pasadena, California

1971

(Submitted May 28, 1971)

ACKNOWLEDGMENT

It is with much pride that I acknowledge Professor Theodore Yao-tsu Wu for his brilliant and inspiring guidance during the years of my graduate study at Caltech. I owe him many debts of gratitude but specifically I would like to thank him for suggesting this interesting problem and also for providing me with pre-copies of his monumental work [1] which served as a model for this problem.

I feel singularly fortunate to have been selected as the recipient of a Naval Ship Research and Development fellowship and later a National Science Foundation traineeship during my tenure here. The former was made possible largely by Dr. W. E. Cummins, Director of the Ship Performance Dept. of N. S. R. D. C., to whom I shall forever be grateful. I would also like to acknowledge Drs. Nils Salvesen, Choung Lee, and Nick Newman, for I feel that their friendship and enthusiasm directly or indirectly guided me into the happy experience that I have enjoyed at Caltech.

I wish to thank Dr. Chris Brennen for his interest in this work and for his many valuable suggestions. A hearty thank you to Mrs. Barbara Hawk (who so generously donated much of her own time) and Mrs. Virginia Conner for typing the manuscript and Miss Cecilia Lin for drawing the figures.

Words cannot adequately describe the debt to my wife. Her encouragement, enthusiasm, and love during every step of the way have always been noticed and cherished. To her I dedicate this thesis.

ABSTRACT

A hydromechanical theory is developed for cycloidal propellers for two limiting modes of operation wherein $U \gg \Omega R$ and $U \ll \Omega R$, with U the rectilinear propeller speed (speed of advance) and ΩR the rotational blade speed. A first order theory is developed from the basic principles of the kinematics and dynamics of fluid motion and proceeds from the point of view of unsteady hydrofoil theory.

Explicit expressions for the instantaneous forces and moments produced by blade motions are presented. On the basis of these results an optimization procedure is carried out which minimizes the energy loss under the constraint of specified mean thrust. Under optimal conditions the propeller is found to possess high Froude efficiencies in both the high and low speed modes of propulsion. This efficiency is defined as the ratio of the average useful work obtained during one cycle of propeller operation to the average power input required to sustain the motion of the propeller during the cycle.

TABLE OF CONTENTS

Chapter	Title	Page
	Acknowledgments	ii
	Abstract	iii
I.	INTRODUCTION	1
II.	KINEMATICS OF THE MOTION	
	1. Coordinate systems and qualitative description of the flight path	6
	2. Definition of the "mean angular position"	8
	3. Trajectory equations	9
	4. Boundary condition on the blade	12
	5. The nature of the fluid disturbance	13
	6. Limiting cases for a small perturbation theory	15
III.	A SMALL PERTURBATION FOR CYCLOIDAL PROPELLERS	
	1. Development of the equation of motion	19
	2. Vorticity in the field	21
	3. Continuity of $F = \bar{\phi} + i\Psi$ across a free vortex sheet	22
	4. Integration of the Euler equation	23
	5. The Riemann-Hilbert boundary value problem for f	28
	6. A simple path of integration	32
	7. Evaluation of $a(\tau)$	35
	8. Leading-edge suction	36
IV.	FORCES, POWER AND ENERGY BALANCE	
	1. Forces and moments	38

Chapter	Title	Page
	2. Energy	41
	3. Power input	44
	4. Long time approximation of $a(\tau)$	45
	5. Limiting cases of the motion; Time averaged results	46
V.	OPTIMIZATION	
	1. Specification of the blade motion	49
	2. The effective harmonic blade motion	50
	3. Non-trivial blade motion with vanishing \bar{E} , \bar{T} , and \bar{P}	51
	4. The optimal problem	53
	5. Development of thrust	56
	6. Efficiency	56
	7. Multiple blades	58
VI.	SUMMARY AND DISCUSSION	60
	APPENDIX	67
	REFERENCES	70

I. INTRODUCTION

A cycloidal propeller is a propulsive device that consists of a number of high-aspect-ratio blades of uniform cross section which revolve in a circular orbit about a central axis while the axis moves in a transverse direction in forward motion. The blades are placed at regular intervals along a disc of radius R and are permitted to pitch about a spanwise blade axis. These blades are typically of airfoil shape, usually without camber. They may terminate at one or both spanwise ends by an end plate perpendicular to the propeller axis. See Fig. 1.

Owing to the features that the blades have a high-aspect-ratio and constant cross sections and particularly in the case when the end plates are present, a two dimensional analysis in the plane transverse to the central axis is expected to provide a good approximation to the quantitative results. The simplest case of a single bladed cycloidal propeller is considered but the results may be extrapolated to multi-bladed systems provided the number of blades is limited to the extent that the mutual interference between the blades is small and can be neglected. This limiting case corresponds to the situation when the chord of the blades is small compared to the gap between consecutive blades, or more specifically, when $Nc \ll 2\pi R$, where N is the number of blades, each having chord c .

Cycloidal propellers are lift oriented propulsive devices which derive their versatility from judicious selections of blade attitude relative to their trajectory. They are not to be confused with the

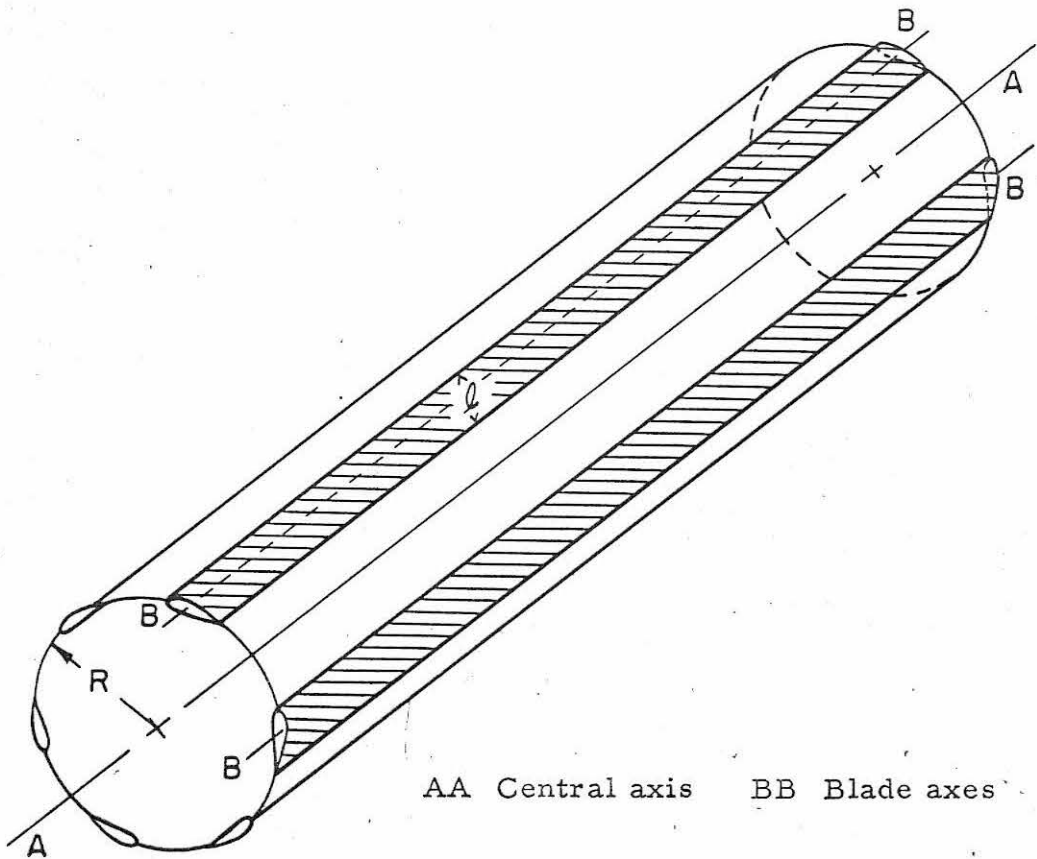


Fig. 1 Schematic representation of a cycloidal propeller. When the central axis experiences an angular velocity Ω then each blade will respond with a speed ΩR relative to the axis.

inefficient drag oriented propellers which fall into the paddle wheel category.

The purpose of this study is to present a consistent and unified hydromechanical theory for a general class of cycloidal propeller. A uniformly valid first order theory is developed from the basic principles of the kinematics and dynamics of fluid motion. The investigation proceeds from the point of view of unsteady hydrofoil theory and adopts many of the ideas exemplified in T. Y. Wu's current treatise on the hydromechanics of swimming propulsion[1].

When the instantaneous forces and moments produced by blade motions are known, it becomes possible to optimize blade attitude on the basis of a number of desirable isoperimetric conditions. An optimization is carried through which minimizes the energy loss under the constraint of specified thrust.

For purposes of the present investigation the blade speed is assumed to be small enough to treat the fluid as incompressible. The characteristic Reynolds number, based on the blade speed and the chord length, however, will be assumed to be large. The presence of a boundary layer along the blade surface is confined to a narrow region and further manifests itself in a thin wake region down stream of the trailing edge. The boundary layer proper is neglected and a free vortex sheet is taken to represent the effects of viscosity in the wake. The problem thus is one of a potential flow.

Previously the propeller based on this principle, or with further variations, has been employed in a low speed propulsion mode, primarily on marine vehicles operating in restricted waters. Due to

the propeller's wide range of thrust orientation, namely, over a complete 360° phase, ship maneuverability can be greatly enhanced. This feature may render the conventional rudder obsolete, thus providing simplifications in stern design.

This paper deals with both the high and low speed modes of propeller operation and presents the optimal blade motions which are associated with maximum Froude efficiencies quite near unity. A more detailed theory which accounts for three dimensionality, the mutual interaction between blades, and the effect experienced by a blade passing through a vortex sheet (shed by a preceding blade) would yield more accurate results.

The wake crossing phenomenon is pertinent to the low speed mode of propulsion where presumably a gust situation would be encountered. Admittedly we neglect the wake crossing effect but we do so advisedly since the blade otherwise perceives a uniformly quiescent field. A more crucial situation involves the distribution of vorticity at the trailing edge of the blade and its effect on the thrust producing capabilities of the propeller. This vorticity is always present in the immediate vicinity of the blade (except when the blade motion is such that the circulation about it remains constant) and the subsequent theory takes this aspect into account.

Some previous investigations (e. g. [4], [5]) of the cycloidal propeller have taken a quasi-static approach to this hydrodynamical problem. Such a theory regards the forces and moments to be those obtained as if the propeller travels in a steady state at the appropriate

instantaneous relative velocity. This approach altogether misses the unsteady contributions associated with the "virtual mass" and the "virtual moments of inertia" of the fluid, and, even more severely, the unsteady component of the singular leading-edge suction which may vary with the reduced frequency of the motion, and may become greater, by several orders of magnitude than its steady value.

Other investigators (e.g. [6], [7]) have tried to extract the details of the blade motion from what amounts to a far field representation of the flow. Here the main idea is to vary a "bound vorticity function" in such a manner that the energy loss is as small as possible under the constraint of specified mean thrust. Once the so-called "optimum bound vorticity function" is known, the blade attitudes are obtained by relating this function to the kinematic boundary condition on the blade. The proposition suffers the same fate as a quasi-static approach since the picture is blurred in the immediate vicinity of the blade. It is here where the interesting physics associated with the acceleration of fluid about the blade's leading edge, the fluid accelerations accompanying transverse blade motions and the distribution of vorticity at the trailing edge occurs. The literature on the subject is extensive. References [4] through [10] seem to be representative of the more recent work.

II. KINEMATICS OF THE MOTION

1. Coordinate systems and qualitative description of the flight path.

A blade will traverse a cycloidal path relative to a frame of reference (ξ, η) which is fixed with respect to the undisturbed fluid and is itself an inertial frame. We also define a "blade coordinate system" (ξ', η') with the origin fixed at the central axis of the propeller and with the η' -axis passing through the pitching-axis of a certain blade in question. Consequently in this translating and rotating frame of reference, the coordinates (ξ', η') will describe the pitching motion of a blade relative to the ξ' -axis. The pitching axis of the blade is along the positive η' -axis at a fixed distance R from the origin. Finally we introduce another frame of reference termed the "body coordinate system" (x, y) with the origin at the blade pitching axis and with the x -axis containing the blade chord (or the mean position of the blade chord). We denote the unit base vectors associated with the three coordinate systems, $\underline{\xi}$, $\underline{\xi}'$, and \underline{x} by \hat{e}_i , e'_i and e_i ($i = 1, 2$) respectively. See Fig. 2.

The cycloidal path is achieved if one observes from the inertial frame the blade's motion due to the combined action of a constant angular velocity Ω and a steady rectilinear speed U of the central axis. However, the cycloidal path assumes quite different appearances depending upon the relative sizes of the two characteristic propeller velocities U and ΩR . For example, if the rectilinear velocity U is large compared with the rotational velocity ΩR then the blade trajectory is very nearly sinusoidal, resembling the

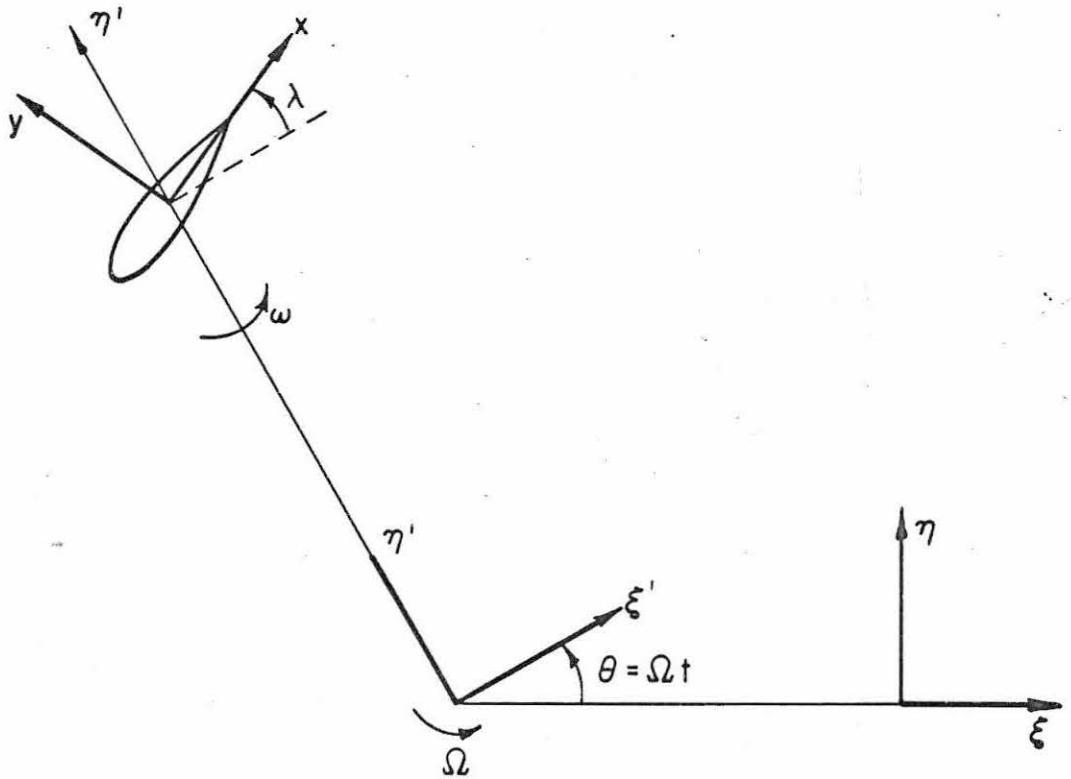


Fig. 2 (Illustration of the inertial coordinate system (ξ, η) , blade coordinate system (ξ', η') and body coordinate system (x, y) where the central axis is assumed to have a constant angular velocity Ω and a constant translational speed U in the negative ξ -direction. The time dependence of λ and ω are specified in §2).

oscillatory path traversed by a fish tail when the creature progresses in straight line flight. Formally, the curve is a curtate cycloid.* In the opposite case of $\Omega R > U$ the blade path circulates about in an overlapping path called a prolate cycloid.* When $U = \Omega R$, the curve generated is called a common cycloid.

2. Definition of the "mean angular position".

Since the flight path is completely established upon fixing the rectilinear and rotational velocities, the motion of the propeller is completely described when further given the angular orientation of a blade relative to its trajectory. The angular orientations of the other blades are then determined by the periodicity with respect to the reference blade. The angular velocity of the reference blade about its pitching axis is specified in accordance with the following requirement. First, a particular reference state of operation is defined as one in which each blade follows its trajectory so that its chord is always tangential to the flight path at its mid-chord. We shall refer a propeller to such a state by saying that it occupies a "mean angular position" along its path. We can then prescribe the angular displacement, λ , of the blade and its angular velocity, ω , both referred to the "mean angular position".

$$\operatorname{tg}(\lambda) = \frac{-\sin \theta}{(\cos \theta + \Omega R/U)} , \quad (1)$$

$$\omega = \dot{\lambda} + \Omega , \quad (2)$$

*cf. Mathematics Dictionary edited by G. James and R. James, Van Nostrand Company, Inc.

where $\theta = \Omega t$ and the dot over λ indicates differentiation with respect to the time t .

The velocity of the origin of the body system relative to the fixed inertial system can be expressed as $\underline{V} = -V \underline{e}_1$, where \underline{e}_1 is the unit vector tangential to the flight path and V in fact becomes the rectilinear speed of the blade in its "mean angular position."

$$V = [U^2 + (\Omega R)^2 + 2U\Omega R \cos \theta]^{\frac{1}{2}} \quad . \quad (3)$$

Motions of a blade following the prescription given by Eqs. (1), (2) lead to far reaching implications, since intuitively, when a blade exercises a "small" deviation (compared with the half chord length) away from its "mean angular position" it generates only "small" perturbations in the surrounding fluid provided the curvature of the trajectory is sufficiently mild. This notion is rigorized in §5 and upon it rests the validity of a linearized approach to the hydrodynamical considerations.

3. Trajectory equations.

In this section a parametric representation of the trajectory is obtained.

We let the position vector $\underline{s}(t)$ follow the progress of the blade (more precisely, its mid-chord) in the fixed inertial system as a function of time. If the propeller is assumed to be at rest for $t < 0$ and for $t > 0$ to have a velocity $\underline{V} = (\underline{U} + \underline{\Omega} \times \underline{R})$, then at time t the location of the blade is given by

$$\underline{s}(t) = \int_0^t \underline{V}(t') dt' + \hat{e}_2 R \quad (4)$$

Vector $\underline{x}_0(t';t)$, defined as the difference between the position vector \underline{s} at times t' and t , reads

$$\underline{x}_0(t';t) = \int_t^{t'} \underline{V}(t') dt' \quad (5)$$

The interpretation of \underline{x}_0 is obvious from Fig. 3.

Resolving \underline{x}_0 into the body system components yields the desired parametric representation of the trajectory

$$x = x_0(t';t) = - \int_t^{t'} V(t') \cos [\nu(t';t)] dt' \quad (6)$$

$$y = y_0(t';t) = - \int_t^{t'} V(t') \sin [\nu(t';t)] dt' \quad (7)$$

where

$$\nu(t';t) = \int_t^{t'} \omega(t') dt' \quad (8)$$

The curvature κ of the flight path is easily calculated from (6), (7), and (8). Interestingly it takes the form of a ratio of the two velocities which characterize the blade motion in the "mean angular position",

$$\kappa(t') = \frac{\omega(t')}{V(t')} \quad (9)$$

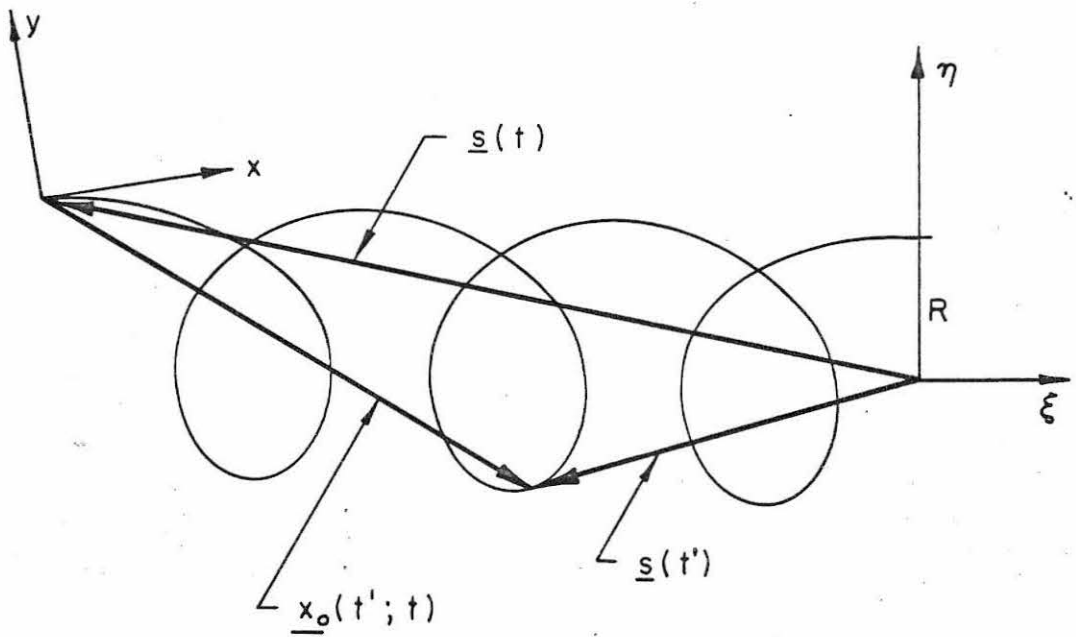


Fig. 3 $\underline{x}_0(t'; t) = \underline{s}(t') - \underline{s}(t)$ traces a trajectory (prolate cycloid) of the blade axis in the body system with t' as parameter.

4. Boundary condition on the blade.

The boundary condition on the blade relates the fluid velocity at the blade surface with the blade's transverse motions. The specific connection is conveniently developed using the body system as reference. The velocity due to the relative motion between the inertial and body systems is

$$\underline{c} = \underline{V} + \underline{\omega} \times \underline{x} \quad (10)$$

where \underline{x} (position vector in the body system) gives the location of the point whose velocity is desired. The absolute velocity of a fluid particle is expressed in terms of the velocity as seen in the body system, \underline{w} , and the relative velocity \underline{c} as

$$\underline{q} = \underline{w} + \underline{c} \quad (11)$$

For engineering purposes it is sufficient to represent the blade motion by the transverse displacement of its mean chord line $y=h(x, t)$ with x and t ranging in intervals to be specified later. Here, we shall neglect the secondary effects of blade thickness. To avoid a point of confusion the body frame is now being used as a reference to describe deviations of the blade away from its "mean angular position."

Suppose that $y = h(x, t)$ is known. Then the blade's normal velocity (relative to the body frame) is given by $\frac{\partial}{\partial t} h(x, t)$ and this $\frac{\partial}{\partial t} h(x, t)$ must be equal to the normal velocity of the fluid (as seen in the body frame), $\underline{w} \cdot \underline{n}$. Here $\underline{n} = \frac{\nabla(h-y)}{|\nabla(h-y)|}$ is the unit vector normal to $y = h(x, t)$. The equivalence of the two normal velocities gives a

statement of the kinematic boundary condition which may be written

$$\frac{d}{dt}(h-y) = \frac{\partial h}{\partial t} + (\underline{w} \cdot \nabla)(h-y) = 0 \quad \text{on } y = h(x, t) \quad (12)$$

The equation $y = h(x, t)$ can also be given parametrically.

With t' as parameter, (12) assumes the form

$$(x_t - w_1)y_{t'} - (y_t - w_2)x_{t'} = 0 \quad (\text{on } x = x(t';t), \quad y = y(t';t)) \quad (12')$$

with $\underline{w} = (w_1, w_2)$ given in (11).

5. The nature of the fluid disturbance.

Consider the motion of a flexible body of negligible thickness which executes transverse motions along an arbitrary flight path. If the flexible body for all times coincides with the flight path at all points along its entire body length then the body will in no way disturb the inviscid fluid. Since in potential flow there is no mechanism by which to transmit a shear stress, such a body essentially slips along its trajectory. The proof that no disturbance prevails follows from the boundary condition on the flexible body, the state of the fluid motion at infinity together with the inviscid irrotational nature of the flow.

Instead of an arbitrary flight path we specialize for the moment to the trajectory of Eqs. (6), (7). For t' ranging in some interval, we think of (6), (7) as describing the motion of a flexible body. Substituting in the kinematic condition (12') yields

$$v/u = tg(\nu) \quad (\text{on } x = x_o(t';t), \quad y = y_o(t';t)) \quad (13)$$

where u, v are the x, y components of the absolute velocity \underline{q} and

v is given by (8). Equation (13) implies that the flow is everywhere tangential to the flexible body surface, a fact which manifests itself in the linear dependence of the absolute velocity components.

The unit vector normal to the trajectory is

$$\underline{n} = \sin \nu \underline{e}_1 - \cos \nu \underline{e}_2 \quad (14)$$

Along the surface that defines the trajectory we have

$$\frac{\partial \varphi}{\partial \underline{n}} = \underline{q} \cdot \underline{n} = u n_1 + v n_2 \quad \text{and use of (13) and (14) gives}$$

$$\frac{\partial \varphi}{\partial \underline{n}} = 0 \quad (\text{on } x = x_0(t';t), \quad y = y_0(t';t))$$

where φ is the velocity potential such that $\underline{q} = \underline{\nabla} \varphi$.

Initially the fluid is quiescent. Any subsequent disturbance is assumed to decay at infinity so that on a surface at infinity which joins the beginning of the trajectory with the end, we have

$$\frac{\partial \varphi}{\partial \underline{n}} = 0 \quad \text{on } S_\infty$$

The field equation is the Laplacian $\nabla^2 \varphi = 0$, valid in a domain defined by boundaries upon which the normal derivative of φ vanishes. This is the classical Neumann boundary value problem and by the uniqueness theorem associated with it, φ is at most a constant throughout the domain. Therefore $\underline{q} = \underline{\nabla} \varphi = 0$ everywhere in the fluid and the proof is complete.

Suppose instead of a flexible body we again consider $y=h(x,t)$ as describing the unsteady motions of a rigid blade relative to its trajectory. If we confine our attention to only those trajectories

whose maximum curvature is small compared with the blade's half-chord length l , then small departures from the "mean angular position" will impart only small disturbances to the fluid. In the present investigation the propeller geometry is normalized with respect to the half-chord. The radius R (a measure of the separation between the central axis and blade) is taken to be much greater than unity, a situation which is of practical interest. On this normalized basis, $R \gg 1$ is representative of the particular propeller we have in mind. The foregoing geometric condition has important consequences and we state it explicitly,

$$l = 1 \quad ; \quad R \gg 1 \quad . \quad (15)$$

Condition (15) implies that the blade in its "mean angular position" closely approximates the appropriate segment of the trajectory along all of its chord length provided the curvature κ of the path is not too large.

6. Limiting cases for a small-perturbation theory.

The subsequent analysis is valid only for small disturbances and consequently we must confine the blade motions accordingly. Two limiting cases of the trajectory are considered wherein $U \gg \Omega R$ (Case I) and $\Omega R \gg U$ (Case II). We exclude in the present investigation the case of $U \approx \Omega R$ because there exist in this case isolated regions of large trajectory curvature. Apparently large scale disturbances are unavoidable at such places even when the rigid blade pursues its "mean angular position". However, over a major portion of a common cycloidal (or nearly common cycloidal) trajectory the analysis is

applicable. For Cases I, II (by (9), (1), (2), (3), (15)) the curvature of the flight path is everywhere small (i. e. $\kappa \ll 1$).

Secondly we restrict the blade variations to $y = h(x, t) \ll 1$. As a consequence, products of the velocity components (u, v) will be small compared with those occurring linearly. In the hydrodynamical development the former may be neglected in comparison with the latter and the absolute velocity \underline{q} is expected to be a small perturbation. Thus the investigation naturally centers around the consequences of small blade deviations away from its "mean position." A further consequence of restricting the blade motions as we have done will become clear in the sequel. The situations of low hydromechanical efficiencies associated with separated flow (and characteristic of stall) are also bypassed. Stall is usually attributed to an excessive angle of attack relative to the incident flow, but as M. J. Lighthill points out,^{*} this phenomena may equally well find its origin in an excessively large leading edge suction force. In unsteady thin airfoil theory the leading edge suction can become so large that the accelerated flow finds it impossible to negotiate the corner and subsequently separates. Leading edge suction has an interesting role in the ensuing development and in this inviscid flow theory its magnitude is determined and examined. Apparently nowhere does it exert an overbearing influence and we concluded that the degree of interplay between blade pitching and the blade path alone is insufficient to lead to a crucial situation concerning

* See Ref. 3 §5 - - specifically pp. 298 - 299.

this singular force, since the suction force also depends on the reduced frequency of the motion.

We conclude the section by quoting a form of the kinematical boundary condition on the blade which will be most convenient for later use. However, before doing so, we list the essential steps employed in its derivation.

- (i) Start with the kinematic condition (12).
- (ii) Use the velocity expressions (10), (11) in (12).
- (iii) $y = h(x, t) \ll 1$. The boundary condition may be applied on $y = 0; |x| < 1$.
- (iv) Neglect products of small quantities.

The resulting expression for the component of the perturbation velocity normal to the blade is

$$v(x, y, t) = \left(\frac{\partial}{\partial t} + V(t) \frac{\partial}{\partial x} \right) h(x, t) + \omega(t)x \quad (\text{on } y = 0^\pm, |x| < 1, t > 0) \quad (16)$$

$\frac{\partial h}{\partial t}$ is the normal velocity of the blade which results from the motion when the blade exercises a local time variation away from its "mean angular position." The partial derivative $\frac{\partial}{\partial t}$ appearing in this term represents a time variation measured in the body frame and not in the inertial frame. Suppose the blade assumes an attitude other than the "mean angular position" as it glides along the trajectory with speed V . Fluid is then pushed laterally by the blade at a rate equal to $V(t) \frac{\partial h}{\partial x}$. As a consequence of a curved flight path together with the rigidity of the blade, the blade communicates a disturbance even when it flies at

the "mean angular position". This effect produces a normal velocity given by the $\omega(t)x$ term of (16).

III. A SMALL PERTURBATION FOR CYCLOIDAL PROPELLERS

1. Development of the equation of motion.

In an incompressible flow field devoid of external forces and internal viscosity, the principle of conservation of momentum leads to Euler's equation wherein the pressure gradient is balanced by the fluid acceleration,

$$\underline{a} = - \frac{1}{\rho} \underline{\nabla} p \quad (17)$$

The equation is valid in any inertial frame. \underline{a} , the absolute acceleration, measures the rate of change of \underline{q} following a particle. Because of the incompressibility, the hydrodynamic pressure plays only a hydromechanical role. Finally, the del-operator $\underline{\nabla}$ appearing is $\frac{\partial}{\partial \underline{\xi}}$.

In the non-inertial body system the acceleration can be written as

$$\underline{a} = \frac{\partial}{\partial t} \underline{q} + \frac{1}{2} \underline{\nabla}(\underline{q} \cdot \underline{q}) - \underline{\nabla}(\underline{q} \cdot \underline{c}) \quad ; \quad \underline{\nabla} = \frac{\partial}{\partial \underline{x}} \quad (18)$$

The term $\frac{\partial}{\partial t} \underline{q}$ measures the instantaneous time variation of \underline{q} with respect to the body system. The term $1/2 \underline{\nabla}(\underline{q} \cdot \underline{q}) = (\underline{q} \cdot \underline{\nabla}) \underline{q}$ is a convective acceleration which arises due to spatial changes of \underline{q} . The last term of (18), $\underline{\nabla}(\underline{q} \cdot \underline{c})$, can be decomposed into the sum of two accelerations, one of which is a convective acceleration (convected at the relative velocity \underline{c}) and the other a Coriolis acceleration $(\underline{q} \times \underline{\omega})$.

Since the spatial derivatives of scalar quantities remain invariant under the transformation from the inertial to body system, the balance of pressure gradient with the fluid acceleration takes the

following form in the non-inertial body system

$$\frac{\partial}{\partial t} \underline{q} + \nabla \left(\frac{1}{2} \underline{q}^2 - \underline{q} \cdot \underline{c} \right) = - \frac{1}{\rho} \nabla P \quad (19)$$

Again, to emphasize, all derivatives are performed in the body frame. Equation (19) and the continuity equation $\text{div} \underline{q} = 0$ provide the equations of motion.

Expressing the absolute velocity as the gradient of a scalar potential φ , it becomes possible to obtain a first integral of (19). Upon absorbing an unessential arbitrary function of time into the velocity potential and neglecting the quadratic perturbation velocity term, (see Chapter II, §6) the result of the integration reads

$$\left(\frac{\partial}{\partial t} + V \frac{\partial}{\partial x} \right) \varphi + \omega \left(y \frac{\partial}{\partial x} - x \frac{\partial}{\partial y} \right) \varphi = \Phi \quad (20)$$

where Φ , Prandtl's acceleration potential, measures the variation of pressure from the hydrostatic level

$$\Phi = \frac{P_{\infty} - P}{\rho} \quad (21)$$

Equation (20) indicates that the momentum imparted to the fluid arises from three sources, namely,

- (i) time varying blade motions relative to the "mean position"
- (ii) rectilinear blade motions
- (iii) angular blade motions.

That pressure variations arise from three such mechanisms seems eminently reasonable.

Operating on the linearized equation (20) with the Laplacian

operator ∇^2 and using $\text{curl } \underline{q} = 0$ and $\text{div } \underline{q} = 0$ yields

$\nabla^2 \Phi = \Phi_{xx} + \Phi_{yy} = 0$. Therefore a function conjugate to the acceleration potential exists (call it Ψ) such that the Cauchy-Riemann equations $\Phi_x = \Psi_y$, $\Phi_y = -\Psi_x$ are satisfied. Since both the velocity and acceleration potentials are analytic functions, we expect the complex-variable theory to prove very useful in the following development. However, before pursuing a solution to the equations of motion, we pause to establish some ideas concerning the shedding of vorticity into the field and to develop some further properties of the acceleration potential.

2. Vorticity in the field.

As we have already mentioned, the wake behind the blade is represented by a free vortex sheet. Mathematically, such a sheet is characterized by a surface across which the tangential velocity is discontinuous whereas all other physical quantities remain continuous. Specifically, a free vortex sheet can not support a pressure difference and should one be imposed, the sheet would reposition itself so as to eliminate that difference.

It is well known that vortex elements interact establishing a secondary flow phenomenon which acts to convect the vorticity from where it was originally located. In this work the blade speed is always much greater than any subsequent vorticity displacement rate. Consequently we neglect the convection of vorticity. In addition, we take the vorticity to lie along that part of the trajectory which has been traversed by the projection of the blade's trailing edge. Hence, insofar as the distribution of vorticity is concerned, we are neglecting the

small wavy motions of the blade which are superposed on the flight path.

The strength of the vortex sheet is tied in with the communication of angular momentum to the fluid as a result of non-uniformities in blade motion. Commensurate with the addition of angular momentum due to blade unsteadiness is the appearance of vortex shedding at the trailing edge. The production of vorticity represents a supply of angular momentum in the sense opposite to that which the fluid experiences as a result of non-uniform blade motion. This in turn becomes the necessary ingredient for the conservation of angular momentum.

3. Continuity of $F = \Phi + i\Psi$ across a free vortex sheet.

Of particular interest to us is the behavior of the function conjugate to the acceleration potential across the free vortex sheet. In fact the successful application of the technique employed in solving the equation of motion hinges on the continuity of Ψ in the flow field. For this reason the following demonstration of its continuity is presented.

By physical requirement the pressure is continuous across a free vortex sheet. Consequently, Φ is unaware of the presence of free vorticity. (For this reason there is a definite advantage to working with Φ as opposed to the velocity potential which experiences a discontinuity across a vortex sheet).

Since Φ is an analytic function it is not only continuous everywhere in the flow field but further it is continuously differentiable

everywhere except across the blade. Furthermore, since the conjugate function Ψ is likewise an analytic function in the same domain as Φ , it too will remain continuous across a free vortex sheet. We define the complex acceleration potential by

$$F(z, t) = \Phi(x, y, t) + i\Psi(x, y, t) \quad (22)$$

where $i = (-1)^{\frac{1}{2}}$ is the imaginary unit and $z = x + iy$. We know that the function F remains continuous for all values of $z = x + iy$ provided the region occupied by the blade is excluded.

4. Integration of the Euler Equation.

The linearized version of the equation of motion (19) may be cast into the following complex-variable form

$$\frac{\partial}{\partial z} F(z, t) = \left(\frac{\partial}{\partial t} + V(t) \right) w - i\omega(t) \frac{\partial}{\partial z} (zw) \quad (23)$$

where $w = u - iv$ is the complex-variable representation of the absolute velocity, \underline{q} . No confusion should arise with the vector \underline{w} which has been used previously for a different purpose.

Of the two velocities which directly characterize blade motion, $V(t)$, $\omega(t)$, the rectilinear speed V dominates the rotational blade speed ωx ; ($|x| < 1$). Were this not the case, the curvature of the flight path would no longer remain small. (Refer back to Chapter II, § 6). It is convenient to fashion (23) to reflect the relative roles of the characteristic blade velocities. We do so by introducing a new measure of time. Let τ be a new 'time' variable (or more precisely the arc length traversed along the flight path in time t) such that

$$\tau = \tau(t) = \int_0^t V(t') dt' \quad (24)$$

Since V is assumed to be positive semi-definite, (24) provides a one to one mapping between t and τ whose inverse $t = t(\tau)$ exists and is a well behaved monotonically increasing function. Regarding w and F as functions of z and the new variable τ , we obtain from (23) upon multiplying with $1/V(t)$ another form of the equation of motion.

$$\frac{\partial}{\partial z} f(z, \tau) = \left(\frac{\partial}{\partial \tau} + \frac{\partial}{\partial z} \right) w(z, \tau) - i\kappa(\tau) \frac{\partial}{\partial z} (zw) \quad (23')$$

where $f(z; \tau) = \frac{F(z, t)}{V(t)}$ has been introduced and $\kappa(\tau) = \frac{\omega(t(\tau))}{V(t(\tau))}$ is the curvature function (see (9)). Note that by normalizing the equation of motion on the bases of the rectilinear blade speed the term pertinent to the curvilinear motion is multiplied by a small coefficient which in fact is the curvature of the blade path.

We solve (23') for w in terms of f by the method of characteristics. The characteristic curve to this equation is obtained upon integrating

$$\frac{dz}{d\tau} = B(z, \tau) = 1 - i\kappa(\tau)z \quad (25)$$

With some manipulation the result of this integration may be expressed as

$$z' = z'(\tau'; z, \tau) = [z - z_0(\tau'; \tau)] e^{-i\nu(\tau'; \tau)} \quad (26)$$

where (z', τ') is an arbitrary point of the z, τ space and

$$z_0(\tau; \tau') = x_0(\tau'; \tau) + iy_0(\tau'; \tau) = \int_{\tau'}^{\tau} e^{i\nu(\tau'; \tau)} d\tau'$$

is the equation of the trajectory (6), (7) expressed as a complex-function. $\nu(\tau'; \tau)$ is the same angle given in (8) but here expressed in the new time variables τ, τ' . For convenience we will re-write it

$$\nu(\tau'; \tau) = \int_{\tau}^{\tau'} \kappa(\tau') d\tau' \quad . \quad (8')$$

A derivation of (26) is presented in Appendix I.

The shape of the characteristic curve (26) may easily be envisioned in the following way. Suppose z, τ to be specified. Then by permitting τ' to range from τ to τ_0 we trace the subsequent path of z' . The curve will originate at the point z . Furthermore, it attempts to imitate the pattern established by the trajectory but suffers a modulation given by the $e^{-i\nu}$ term. Figure 4 provides a sketch of one possible characteristic.

Performing the integration of the equation of motion along the mathematical characteristics provides an expression for the velocity in terms of the pressure (more precisely the complex acceleration potential). The integration is developed in Appendix I and from there

$$B(z, \tau)w(z, \tau) = f(z, \tau) + \int_{\tau}^{\tau_0} \frac{\partial}{\partial \tau'} f(z', \tau') d\tau' \quad \text{where} \quad (27)$$

$$z' = z'(\tau'; z, \tau) \quad \text{and} \quad z = O(1) \quad .$$

The result has a physical interpretation. The perturbation velocity of a field point at a particular instant of time is related to the

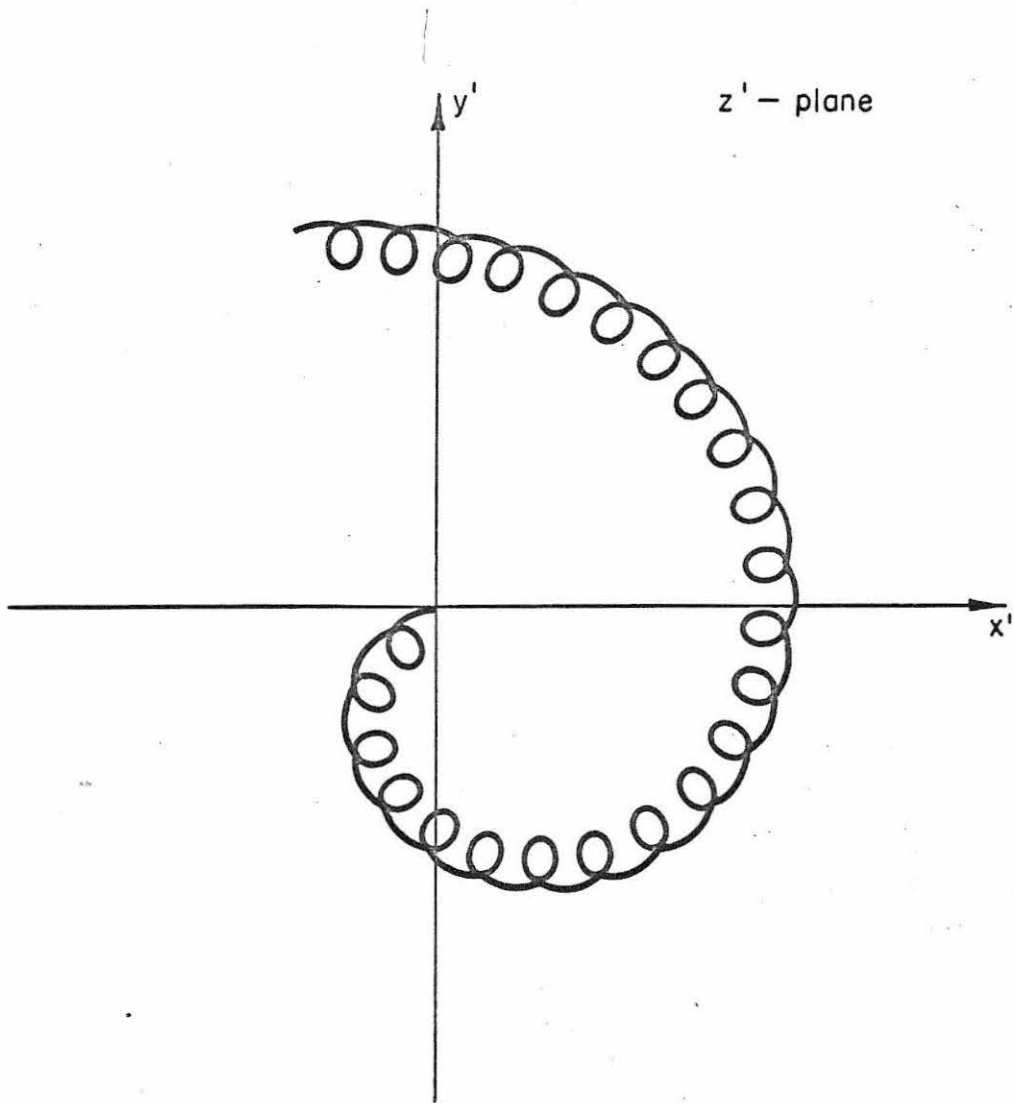


Fig. 4 Characteristic curve emanating from $z = 0$. The curve is representative for propellers having a rotational speed, ΩR greater than the rectilinear speed U .

instantaneous pressure existing at that point plus the summation of all the retarded pressures relevant to a particular curve which emanates from the point. In this sense the fluid may be said to possess a memory. In unsteady problems it is intuitively obvious that previous states of the pressure field must have some bearing on the present state of the velocity field because of the continuous vortex shedding. Equation (27) provides a quantitative statement of the influence.

In finding a solution to the equation of motion we will have need for a different form of integral to (23') wherein f is expressed in terms of w . This may be obtained by directly integrating the equation (23') with respect to z from $z = -\infty$. The result is

$$B(z, \tau)w(z, \tau) = f(z, \tau) - \int_{-\infty}^z \frac{\partial}{\partial \tau} w(z, \tau) dz \quad . \quad (28)$$

In arriving at this result we have tacitly assumed that in the far field ($|z| \rightarrow \infty$):

- (i) the pressure maintains the hydrostatic level ($f \rightarrow 0$).
- (ii) the perturbation velocity decays sufficiently fast. If the flow contains no net source or vorticity then, at most, $w = O(1/|z|^2)$ in the far field. Consequently, $B(z, \tau)w(z, \tau)$ tends to zero there,

The two integrals (27), (28) which we have obtained to the equation of the motion mark some progress toward a full solution. What is lacking in the ultimate pursuit, of course, is a knowledge of the pressure field throughout the flow and for all time. A similar

knowledge of the velocity field would serve equally well via (28).

The determination of the complex acceleration potential forms the subject of the next section wherein a particular function of time arises. From the identity apparent on comparing (27) and (28) we define this function of time by

$$iA(\tau) = \int_{-\infty}^{-1} \frac{\partial}{\partial \tau} w(z, \tau) dz, = \int_0^{\tau} \frac{\partial}{\partial \tau'} f(z'(\tau'; -1, \tau), \tau') d\tau' \quad (29)$$

Note that the last integral is evaluated along the characteristic which emanates from the leading edge. The significance of $A(\tau)$ will become clear when we investigate the leading edge suction.

5. The Riemann-Hilbert boundary value problem for f .

We call the domain D^+ the field of flow and define it to be the region bounded by the blade C and the contour at infinity C_∞ . When C or C_∞ is traversed in the positive direction D^+ will always be on the left hand side. We seek a sectionally holomorphic function $f(z)$ of finite degree at infinity. This function satisfies the following boundary condition on C and C_∞ .

$$f^+(z, \tau) = G(z)f^-(z, \tau) + g(z, \tau) \quad (30)$$

where z is an element of C or C_∞ . $G(z)$ and $g(z, \tau)$ are given. f^+ (f^-) refers to the value of f as z approaches the boundary from above (below) in the case of C . The plus-minus notation is not used here on the contour at infinity. See Fig. 5.

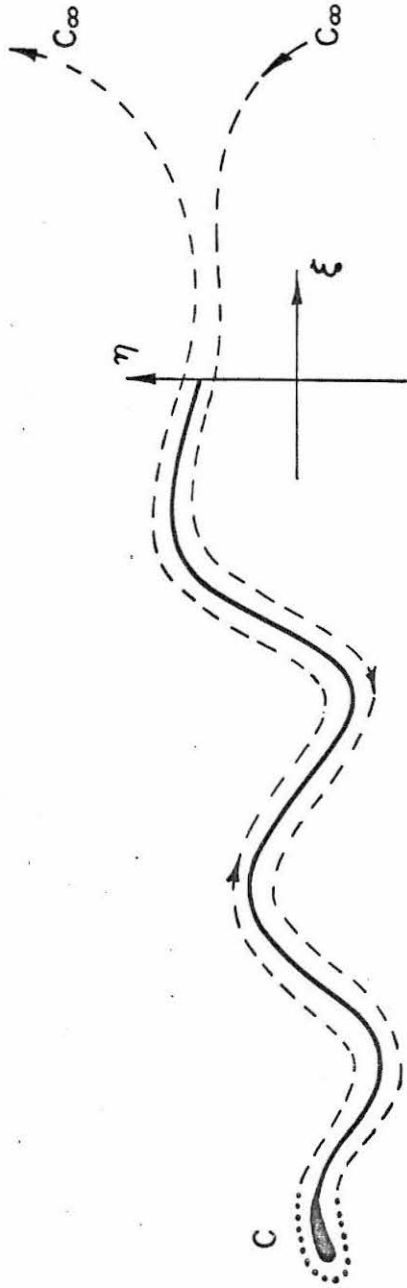


Fig. 5 Representation of the control surface defining D^+ .

The index of the Riemann-Hilbert problem is defined as

$$k = \frac{1}{2\pi i} [\log G(z)]_C + \frac{1}{2\pi i} [\log G(z)]_{C_\infty} \quad (31)$$

where the brackets signify the increment of the function inside as a result of one complete traversal of the indicated contour in the positive direction. For vanishing index there exists only one solution vanishing at infinity. (See e. g. Chapter V of reference [11]). This solution takes the form

$$f(z, \tau) = \frac{H(z)}{2\pi i} \int_C \frac{g(\xi, \tau) d\xi}{H^+(\xi)(\xi - z)} \quad (32)$$

where $H(z)$ is a homogeneous solution satisfying

$$G(\xi) = \frac{H^+(\xi)}{H^-(\xi)} \quad \text{on } C \quad (33)$$

In the past few sections we have explicitly developed or made feasible certain properties of the complex acceleration potential.

Among these are:

- (i) f is an analytic function of $z = x + iy$ for all time.
- (ii) f has a discontinuity across the blade. (Take for C the set $z = x \in [-1, 1]$).
- (iv) f tends to zero at infinity.

For the present purpose we have need for two more conditions on the complex acceleration potential. One is associated with the Kutta-Zhukovskii condition that the flow finds it impossible to negotiate the corner at a sharp trailing edge. We translate this into a condition on f .

(v) f remains bounded at the trailing edge.

The final necessary proposition regarding f concerns its character at the leading edge. In the neighborhood of the leading edge the assumption of small perturbations breaks down since here a stagnation point occurs. Hence, the perturbation velocity is of the order of the incident flow. Using the Bernoulli equation with the non-linear terms present, T. Y. Wu has demonstrated [2] that in the neighborhood of the leading edge f exhibits the same singular behavior as the perturbation velocity. This will also be apparent from §8. It is well known that w has there a square root singularity. Thus:

(vi) f tends to infinity as $[1/(z+1)]^{\frac{1}{2}}$ near the leading edge.

The function $g(x, \tau)$ of (32) serves as an intermediary which carries the 'blade input' to the fluid domain. It is defined here as $g(x, \tau) = f^+(z, \tau) + f^-(z, \tau)$ with $|x| < 1$ and the plus (minus) signifying the approach of z from above (below) the blade. From (29), (30) we obtain

$$g(x, \tau) = 2i[A(\tau) + f_1(x, \tau)] \quad (|x| < 1) \quad (34)$$

$$f_1(x, \tau) = -B(x, \tau)v(x, 0, \tau) - \int_{-1}^x \frac{\partial}{\partial \tau} v(x', 0, \tau) dx' \quad (35)$$

Notice that except for a constant (more strictly a function of time) the "input function" is explicitly known. Later, a close look at the leading edge will determine the input which arises from this area.

Consideration of the homogeneous function $H(z)$ is next in line. By (34) $f^+ + f^- = g$ which implies that $G(z) = -1$. Correspondingly, $H^+(x) = -H^-(x)$ for $|x| < 1$. Keeping in mind conditions (v)

and (vi) we choose as a candidate for the homogeneous solution

$$H(z) = \left(\frac{z-1}{z+1} \right)^{\frac{1}{2}}. \quad (36)$$

This choice for H is defined with a branch cut from the blade's leading edge to its trailing edge and tends to unity at infinity. It provides the proper singular behavior required of f at the leading edge. In addition, the boundedness condition of Kutta-Zhukovskii is suitably satisfied. Since G is a constant the index to the Riemann-Hilbert problem is zero. Hence (32) supplies the solution

$$f(z, \tau) = \frac{1}{\pi i} \left(\frac{z-1}{z+1} \right)^{\frac{1}{2}} \int_{-1}^1 \left(\frac{1+\xi}{1-\xi} \right)^{\frac{1}{2}} [A(\tau) + f_1(\xi, \tau)] \frac{d\xi}{(\xi-z)}. \quad (37)$$

For later use, it is convenient to write the solution in a form which isolates the singularity contribution of the leading edge. By a simple manipulation we can accomplish this

$$f(z, \tau) = iA(\tau) - \frac{i}{2} a(\tau) \left(\frac{z-1}{z+1} \right)^{\frac{1}{2}} + \frac{1}{\pi i} \int_{-1}^1 \left(\frac{z^2-1}{1-\xi^2} \right)^{\frac{1}{2}} \frac{f_1(\xi, \tau)}{(\xi-z)} d\xi \quad (37')$$

where

$$\frac{a(\tau)}{2} = A(\tau) + \frac{1}{\pi} \int_{-1}^1 \frac{f_1(\xi, \tau)}{(1-\xi^2)^{1/2}} d\xi. \quad (38)$$

6. A simple path of integration.

In this section we are guided by physical intuition to make a simplification which renders the subsequent analysis more tractable. We propose to approximate the path of integration of (27) so that the resulting velocity field remains accurate to leading order.

Suppose the motion occurs over a long time interval. The blade projects an influence to the field in the form of pressure waves which travel at the speed of sound (taken here to be infinite). Equation (27) implies that the prevailing velocity at a point is determined by the instantaneous pressure at the point together with certain retarded pressures. However the most influential retarded pressures must be those which occur in the immediate past history. Those further removed should occupy a greatly reduced status effecting a negligibly small change in the instantaneous state of the fluid. Certainly, if this were not so, the problem would appear very difficult indeed. Additional support to this line of reasoning is provided by Karman and Sears work [13] on an airfoil pursuing unsteady motion along a straight line trajectory. There they have calculated the induced vorticity distribution along a thin airfoil due to isolated points of wake vorticity placed at various distances behind the trailing-edge. The strength of the induced vorticity is quite large when the wake vortex is very near the trailing-edge but it diminishes in strength rapidly (except near the leading-edge where it is infinite). In fact, the strength of the induced vorticity relevant to a point vortex placed at one chord length behind the trailing-edge is already an order of magnitude smaller than the corresponding strength when the point vortex is at $(1/40)$ of the chord length behind the trailing-edge. It is useful to recall that it is just this trailing vorticity which connects the "past events" of the flow field with the present state of the fluid.

Mathematically this idea suggests that we may to good

approximation evaluate

$$\int_{\tau}^{\tau'} \frac{\partial}{\partial \tau} f(z', \tau') d\tau'$$

along a simplified path given by

$$z' = z + (\tau' - \tau) + iz \int_{\tau'}^{\tau} \kappa(\tau_1) d\tau_1 + i \iint_{\tau' \tau_1}^{\tau \tau} \kappa(\tau_2) d\tau_2 d\tau_1$$

$$z' = z'(\tau'; z, \tau) = [z + (\tau' - \tau)] [1 + O(i\kappa(\tau' - \tau))] \quad (27')$$

Equation (27') very accurately represents (26) near the point (z, τ) up to distances of the order of the chord length. For distances of $O(R)$ (27') affords a fair representation. For distances greater than $O(R)$ (27') rapidly diverges from the true characteristic.

Consider the retarded pressures appropriate to a characteristic originating at an arbitrary field point. The question is raised to which field point will a characteristic emanate yielding the largest retarded pressures? Equation (37') elects the point $z = -1$ since nowhere else is f so large. If we can show that the velocity is accurately obtained to leading order at $z = -1$ from evaluating

$$\int_{\tau}^{\tau'} \frac{\partial}{\partial \tau} f(z', \tau') d\tau'$$

tegration should provide an even better approximation at other field

points. When $\int_{\tau}^{\tau'} \frac{\partial}{\partial \tau} f(z', \tau') d\tau'$ is evaluated along the linear approxi-

mation to the characteristic, $(z' = z + \tau - \tau')$, and then along a path

which provides a better approximation (e. g. along Eq. (27')), then the difference of the two results will be $O(\kappa)$ times the lowest order result. Hence, since we confine attention only to those trajectories whose maximum curvature is at most $O(1/R)$ then the correction will be of higher order in our attempt to establish a uniformly valid first order solution. Consequently, when the path of integration is along a characteristic we can use (27') instead, to a good approximation.

7. Evaluation of $a(\tau)$.

In §5 the complex acceleration potential was explicitly determined except for the term $a(\tau)$. The present section removes this shortcoming.

Define the Laplace transform by

$$\tilde{a}(s) = \int_0^{\infty} e^{-s\tau} a(\tau) d\tau, \quad (\text{Re } s > 0) \quad (39)$$

Substitution of (37') into (29) provides an integral equation for $a(\tau)$. Taking the Laplace transform of the resulting equation and evaluating the known transforms [12] gives

$$\tilde{a}(s) = \frac{2}{\pi} \int_{-1}^1 \frac{\tilde{v}(\xi, 0, s)}{(1-\xi^2)^{1/2}} [\xi - (1+\xi)\tilde{H}(s)] d\xi \quad (40)$$

where $\tilde{H}(s) = \frac{K_1(s)}{K_0(s) + K_1(s)}$; (K_0, K_1 are modified Bessel functions of the second kind).

The inverse transform provides the solution to the integral equation.

$$a(\tau) = \frac{2}{\pi} \int_{-1}^1 \frac{\xi v(\xi, 0, \tau) d\xi}{(1-\xi^2)^{1/2}} - \frac{2}{\pi} \int_{-1}^1 \left(\frac{1+\xi}{1-\xi} \right)^{1/2} \int_0^{\tau} v(\xi, 0, \tau') H(\tau-\tau') d\tau' d\xi \quad (40')$$

$$H(\tau) = \frac{1}{2\pi i} \int_{\lambda' - i\infty}^{\lambda' + i\infty} e^{s\tau} \tilde{H}(s) ds, \quad (\lambda' > 0)$$

Notice that $A(\tau)$ is known from (38) and (40'). Furthermore, both $a(\tau)$ and $A(\tau)$ depend on the past history of the motion via the convolution integral term. The physical significance of $a(\tau)$ is developed in the following section.

8. Leading edge suction.

The singular force can be obtained by applying the Blasius Theorem with a contour surrounding an ϵ - neighborhood of the leading edge. The asymptotic form of f as $z \rightarrow -1$ is obtained from (37'). Substituting it into (27) gives

$$w(z, \tau) = \frac{a(\tau)}{[2(z+1)]^{1/2}} + O[(z+1)^{1/2}], \quad (z \rightarrow -1) \quad (42)$$

In arriving at (42) an $O(1/R)$ contribution in $B(-1, \tau)$ has been neglected. Applying the result to $X_s - iY_s = \frac{i\rho}{2} \int_{L.E.} w^2 dz$ yields the components

of the singular force directed along the body axis

$$X_s = \frac{-\pi\rho}{8} [a(\tau) + a^*(\tau)]^2; \quad Y_s = 0 \quad (43)$$

Notice that X_s is always negative indicating that the singular force is in fact a local thrust. The asterisk denotes the complex conjugate

(with respect to j , the imaginary unit of the time plane). The leading edge suction is seen to depend on the past history of the motion through $a(\tau)$.

IV. FORCES, POWER AND ENERGY BALANCE

1. Forces and moments.

The resultant force $\underline{R} = \underline{X} + \underline{Y}$ developed by the blade is easily calculated in the body system. Here $\underline{X} = X \underline{e}_1$ and $\underline{Y} = Y \underline{e}_2$ and both X and Y are positive when \underline{R} resides in the first quadrant. When the blade departs from its "mean position" an x-directed force arises from the pressure difference $\Delta p = p^- - p^+$ across the blade. We designate this contribution by X_p where

$$X_p = - \int_{-1}^1 (\Delta p) \frac{\partial h}{\partial x} dx \quad . \quad (44)$$

When Δp and $\frac{\partial h}{\partial x}$ are positively correlated then X_p is negative and corresponds to a local thrust. The total x-component of force is the sum of X_p and the singular force X_s .

The normal force on the blade and the moment about the mid-chord are

$$Y = \int_{-1}^1 (\Delta p) dx \quad . \quad (45)$$

$$M = \int_{-1}^1 x(\Delta p) dx \quad (46)$$

M is positive in the "nose-down" sense. Resolving the resultant force into components along the inertial axes provides the thrust and lift forces

$$T = -X \cos \mu + Y \sin \mu \quad (47)$$

$$L = X \sin \mu + Y \cos \mu \quad (48)$$

When T is positive the force is directed along the negative ξ -axis and is properly termed a thrust. μ is the angle between the x and ξ axes ($= \lambda + \theta$).

The acceleration potential is an odd function across the blade and consequently Δp can be expressed as

$$\Delta p = 2\rho\Phi^+(x, 0, t) \quad (|x| < 1) \quad (49)$$

and from (37') and (35):

$$\Phi^+(x, 0, t) = \frac{1}{2} V(t)a(\tau) \left(\frac{1-x}{1+x} \right)^{\frac{1}{2}} + \frac{1}{\pi} \int_{-1}^1 \left(\frac{1-x^2}{1-\xi^2} \right)^{\frac{1}{2}} \frac{f_1(\xi, t)}{(\xi-x)} d\xi \quad (50)$$

$$F_1(\xi, t) = - \left(\frac{\partial}{\partial t} + V \frac{\partial}{\partial \xi} \right) \int_{-1}^1 v(x_1, 0, t) dx_1 = V(t)f_1(\xi, \tau)$$

For purposes of obtaining more explicit expressions of the force and moment we expand $h(x, t)$ in a Fourier cosine series

$$h(x, t) = \frac{\beta_0(t)}{2} + \sum_{n=1}^{\infty} \beta_n(t) \cos n\varphi \quad (x = \cos \varphi) \quad (51)$$

$$\beta_n(t) = \frac{2}{\pi} \int_0^{\pi} h(x, t) \cos n\varphi d\varphi \quad (n = 0, 1, 2, \dots)$$

We also introduce another Fourier cosine series related to (51) by way of the boundary condition on the blade.

$$[v(x, 0, t) - \omega(t)x] = \frac{1}{2} b_0(t) + \sum_{n=1}^{\infty} b_n(t) \cos n\varphi; (x = \cos \varphi) \quad (52)$$

$$b_n(t) = \frac{2}{\pi} \int_0^{\pi} [v(x, 0, t) - \omega x] \cos n\varphi \, d\varphi \quad (n = 0, 1, 2, \dots)$$

To put the force and moment expressions we seek in the desired form, use of the following theorem proved by T. Y. Wu [1] is very helpful.

Theorem: If the arbitrary functions $f(x)$, $g(x)$ and their derivatives $f'(x)$, $g'(x)$ are continuous in $-1 \leq x \leq 1$, then

$$\int_{-1}^1 f'(x) dx \int_{-1}^1 \left(\frac{1-x^2}{1-\xi^2} \right)^{\frac{1}{2}} \frac{g(\xi) d\xi}{(\xi-x)} = \int_{-1}^1 g'(x) dx \int_{-1}^1 \left(\frac{1-x^2}{1-\xi^2} \right)^{\frac{1}{2}} \frac{f(\xi) d\xi}{(\xi-x)},$$

This theorem can be readily proved by successive integrations by parts and by observing the identity

$$(1-\xi^2)^{-\frac{1}{2}} \frac{\partial}{\partial x} \frac{(1-x^2)^{\frac{1}{2}}}{\xi-x} = - (1-x^2)^{-\frac{1}{2}} \frac{\partial}{\partial \xi} \frac{(1-\xi^2)^{\frac{1}{2}}}{\xi-x}$$

The contributions from the Cauchy principal limits $\xi = x - \epsilon$ and $\xi = x + \epsilon$ cancel out as $\epsilon \rightarrow 0$.

After a number of straightforward (but cumbersome) calculations we obtain

$$X = - \frac{\pi\rho}{2} \left\{ (a+b_0 - \dot{\beta}_0)(a-b_1 + \dot{\beta}_1) + \dot{\beta}_0 \dot{\beta}_1 - \dot{\omega} \beta_2 - 2V\omega\beta_1 + \frac{d}{dt} \sum_{n=1}^{\infty} \beta_n (b_{n+1} - b_{n-1}) \right\} \quad (53)$$

$$Y = \pi\rho V(a-b_1 - \omega) - \frac{\pi\rho}{2} \frac{d}{dt} (b_0 - b_2) \quad (54)$$

$$M = - \frac{\pi\rho}{2} \left[V(a+b_2) + \frac{1}{4} \frac{d}{dt} (b_1 - b_3 + \omega) \right] . \quad (55)$$

If complex notation is used for the Fourier coefficients then the real part of each coefficient must be taken. The dot again signifies $\frac{d}{dt}$.

2. Energy.

Designate by \dot{E} the rate at which energy is imparted to the fluid in a unit of time.

$$\dot{E} = \frac{d}{dt} \int_{D^+(t)} \left(\frac{1}{2} \rho q^2 \right) d^3 \underline{x} . \quad (56)$$

The integration is over the entire fluid region. Using the Euler equation (17) and $\underline{q} \cdot \underline{a} = \nabla(\underline{q}\Phi)$ which follows from it and the divergence free nature of \underline{q} , we convert the volume integral into the following surface integral.

$$\dot{E} = \int_S \rho \Phi \underline{q} \cdot \underline{n} dS . \quad (56a)$$

\underline{n} is the unit outward normal to the fluid. The surface S in this integral must encompass all of the fluid. Specifically we take the path prescribed in Fig. 5. Observing the following properties of the

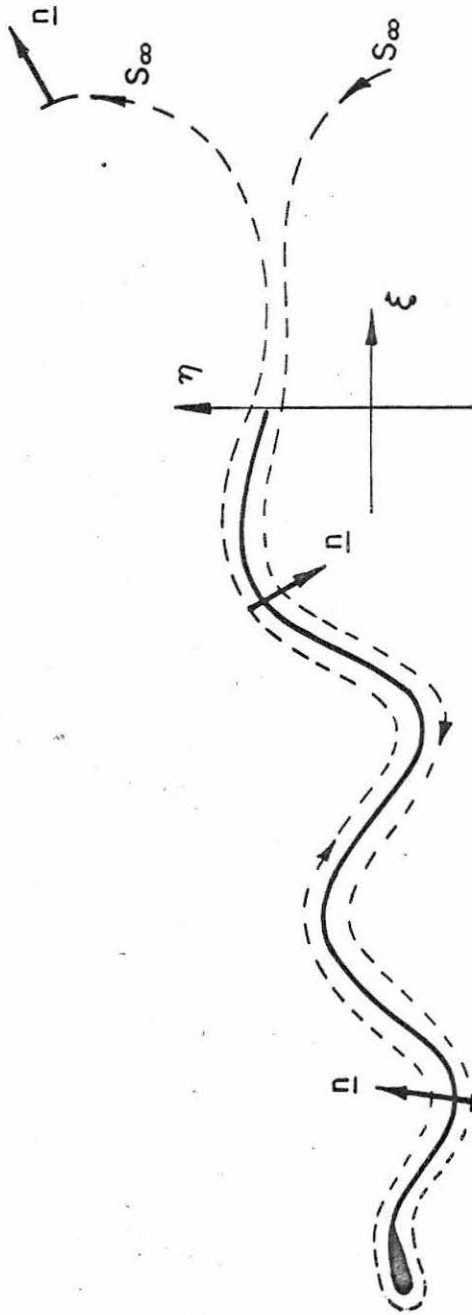


Fig.5 Representation of the control surface defining D^+ .

integrand of (56a) provides another representation of \dot{E} .

- (i) $\underline{q} \cdot \underline{n}$ is continuous across all surfaces.
- (ii) Φ is continuous everywhere except across the blade.
- (iii) Φ and \underline{q} are singular at the leading edge and we therefore expect a contribution to arise from the integration about that point.
- (iv) $\Phi (\underline{q} \cdot \underline{n}) dS \sim O(1/|z|^2)$ in the far field.
- (v) Consider the direction of the normal.

The result we seek is

$$\dot{E} = - \int_{-1}^1 v(x, 0, t) (\Delta p) dx + X_s V \quad (56b)$$

Equations (16), (44), (46) can now be used to express (56b) in still another form.

$$\dot{E} = X V - M \omega - \int_{-1}^1 h_t (\Delta p) dx \quad (56c)$$

Thus, the rate at which energy is communicated to fluid in unit of time arises from:

- (i) the time rate of working of the resultant forces $-\underline{R} \cdot \underline{V} = X V$
- (ii) the time rate of working of the moment $-M \omega$. This is the power required so that the blade can pursue its trajectory in the "mean angular position."
- (iii) the power necessary to deviate away from the "mean position" is supplied by $-\int_{-1}^1 h_t (\Delta p) dx$. Hence, it is the rate of working of the blade against the hydrodynamic reaction opposing lateral blade motions.

Finally we express \dot{E} in terms of Fourier coefficients (with the understanding that the real part is implied in the case of complex coefficients)

$$\dot{E} = \frac{\pi\rho}{2} V [(a+b_0)(b_1 - a + \omega)] + \frac{\pi\rho}{8} \frac{d}{dt} \left[\omega(b_1 - b_3) + \frac{\omega^2}{2} + \sum_{n=1}^{\infty} \frac{1}{n} (b_{n-1} + b_{n+1})^2 \right] \quad (57)$$

3. Power Input

To find the total power we must reflect upon the energy inputs supplied to the propeller to sustain its motion. The rotational velocity imparted to the propeller is generated by the application of a moment M_1 about the central axis. Another moment is applied at the pitching axis of the blade and acts to maintain the "mean position" along the flight path. If, in addition, the blade departs from the "mean position," energy must be added to the blade to overcome the resulting hydrodynamic reaction. Hence, the total power input becomes

$$P = M_1 \Omega - M \omega - \int_{-1}^1 h_t (\Delta p) dx \quad (58)$$

The applied moment at the central axis is equal to the resultant force on the blade projected along the ξ_1 axis times the distance through which it acts. Therefore

$$M_1 = R(X \cos \lambda - Y \sin \lambda) \quad (59)$$

and is positive in the counter-clockwise sense. Combining (56c), (58), (59), (47) and some geometric relationships gives

$$P = UT + \dot{E} \quad (58')$$

As expected the total power input is consumed in two ways, some in generating useful work UT , while the rest is wasted to the fluid.

4. Longtime approximation of $a(\tau)$.

In this development we are not so concerned with the initial motion of the propeller. What is of interest are the circumstances which prevail after the propeller has pursued its periodic course for a long time. Since $a(\tau)$ is the only function appearing in the force, moment, energy, and power expressions which depends on the past history of the motion, we devote this section to finding its long time periodic behavior.

Suppose the motion is prescribed by

$$\left. \begin{aligned} h(x, t) &= \operatorname{Re}[h_1(x)e^{i\alpha\tau}] \\ v(x, 0, t) - \omega(t)x &= \operatorname{Re}[v_1(x)e^{i\alpha\tau}] \\ \omega(t) &= \operatorname{Re}[\omega_0 + \omega_1 e^{i\alpha\tau}] \quad (\omega_0, \omega_1 \text{ constants}) \end{aligned} \right\} (60)$$

Combining (40), (60), (52) gives

$$\tilde{a}(s) = \tilde{\omega}(s) + \frac{b_1}{(s-i\alpha)} - (b_0 + b_1 + \omega_1) \frac{\tilde{H}(s)}{(s-i\alpha)} \quad (61)$$

$\tilde{H}(s)$ has a logarithmic branch point and in the s -plane we place the cut along the negative real axis. The inverse transform gives:

$$a(\tau) = \omega(t) + b_1 e^{i\alpha\tau} - (b_0 + b_1 + \omega_1) e^{i\alpha\tau} \tilde{H}(i\alpha) - \frac{1}{2\pi i} \int_0^{-\infty} (H^+(s) - H^-(s)) \exp \tau(s - i\alpha) \frac{ds}{(s - i\alpha)} \quad (61')$$

Notice that (61') is still exact. Take $\theta = \alpha\tau$. Using a Tauberian theorem ($s \rightarrow 0^+$ corresponds with $\tau \rightarrow \infty$) and applying Watson's lemma to approximate the integral provides the longtime periodic form

$$a(t) = \omega(t) + b_1(t) - \Theta(\alpha) [b_0(t) + b_1(t) + \omega_1(t)] (1 + O(1/\tau^2)); (\tau \rightarrow \infty) \quad (61'')$$

where $\Theta(\alpha) = \Theta_1(\alpha) + i\Theta_2(\alpha) \equiv \tilde{H}(i\alpha)$ is the Theodorsen function whose asymptotic expansion for small α appears next.

$$\begin{aligned} \Theta_1(\alpha) &\sim 1 - \frac{\pi\alpha}{2} + \alpha^2 \left(\frac{\pi^2}{4} - \log^2 \frac{2}{\gamma\alpha} \right) + O(\alpha^3 \log^2 \alpha) \\ \Theta_2(\alpha) &\sim -\alpha(1 - \pi\alpha) \log \frac{2}{\gamma\alpha} + O(\alpha^3 \log^3 \alpha); (\gamma = 1.781\dots) \end{aligned} \quad (62)$$

5. Limiting cases of the motion; Time averaged results

We denote by Case I the high speed made of propulsion where in $U \gg \Omega R$ and by Case II the opposite extreme of $\Omega R \gg U$. Table I presents a collection of some limiting forms assumed by certain geometrical and dynamical quantities belonging to these cases.

TABLE I

<u>Case I ($\epsilon = \frac{\Omega R}{U} \ll 1$)</u>	<u>Case II ($\delta = \frac{U}{\Omega R} \ll 1$)</u>
$\tau \cong U t$	$\tau \cong \Omega R t$
$\alpha = \Omega/U \ll 1/R$	$\alpha = 1/R \ll 1$
$V(t) \cong U + \Omega R \cos \theta$	$V(t) \cong \Omega R + U \cos \theta$
$\omega(t) \cong \frac{\Omega^2 R}{U} \cos \theta$	$\omega(t) \cong \Omega - \frac{U}{R} \cos \theta$
$\omega_0 = 0$	$\omega_0 = \Omega$
$\omega_1 = \frac{\Omega^2 R}{U}$	$\omega_1 = -\frac{U}{R}$
$\kappa(t) \cong \frac{\epsilon^2}{R} \cos \theta$	$\kappa(t) \cong \frac{1}{R} - \frac{2\delta}{R} \cos \theta$
$\lambda(t) \cong -\theta + \epsilon \sin \theta$	$\lambda(t) \cong -\delta \sin \theta$
$\mu(t) \cong \epsilon \sin \theta$	$\mu(t) \cong \theta - \delta \sin \theta$
$L \cong \left(\frac{\Omega R}{U}\right) X \sin \theta + Y$	$L \cong X \sin \theta + Y \cos \theta$
$T \cong -X + \left(\frac{\Omega R}{U}\right) Y \sin \theta$	$T \cong -X \cos \theta + Y \sin \theta$
$a(t) \cong -b_0 + \frac{\Omega}{U} \left(\frac{\pi}{2} + i \log \frac{2}{\gamma \alpha}\right) (b_0 + b_1 + \omega)$	$a(t) \cong \Omega - b_0 + \frac{1}{R} \left(\frac{\pi}{2} + i \log \frac{2R}{\gamma}\right) (b_0 + b_1 + \omega_1)$

An important part of the investigation centers around the steady components of the thrust, energy, and power. In the remainder of this section we present these steady components for Cases I, II.

Consider first the functions $b(\underline{x}, t)$, $c(\underline{x}, t)$ which we assume have expansions of the form

$$b(\underline{x}, t) = \text{Re} \left(\sum_n b_n(\underline{x}) e^{j \omega_n t} \right) \quad ; \quad c(\underline{x}, t) = \text{Re} \left(\sum_n c_n(\underline{x}) e^{j \omega_n t} \right)$$

The time average of the product bc is

$$\overline{bc} = \text{Limit}_{T \rightarrow \infty} \frac{1}{T} \int_0^T b(\underline{x}, t) c(\underline{x}, t) dt = \text{Re} \frac{1}{2} (\sum_n b_n(\underline{x}) c_n^*(\underline{x})) \quad (63)$$

Notice that the steady components pertaining to different frequencies are not coupled. Applying the averaging formula to the expressions for thrust and energy and consulting table I for the appropriate limiting expressions yields for Case I

$$\overline{T} = \frac{\pi \rho}{4} \text{Re} \left\{ (a + b_0 - \dot{\beta}_0)(a^* - b_1^* + \beta_1^*) + \dot{\beta}_0 \dot{\beta}_1^* - \dot{\omega} \beta_2^* - 2U \beta_1 \omega^* + 2 \Omega R i(a - \omega - b_1) - \frac{\Omega R}{U} i(\dot{b}_0 - \dot{b}_2) \right\} \quad (64)$$

$$\overline{\dot{E}} = \frac{\pi \rho}{4} U \text{Re} [(a + b_0)(b_1^* - a^* + \omega^*)] \quad (65)$$

while the average thrust and energy for Case II are

$$\overline{T} = \frac{\pi \rho}{4} \text{Re} \left\{ \Omega [-2 \Omega R \beta_1 + \dot{\beta}_1 - b_1 + b_0 - \dot{\beta}_0 + 2(a - \Omega)] + 2i \Omega R (a - \omega - b_1) + -i(\dot{b}_0 - \dot{b}_2) \right\} \quad (66)$$

$$\overline{\dot{E}} = \frac{\pi \rho}{4} \Omega R \text{Re} \left\{ (a - \Omega + b_0)(b_1^* - a^* + \omega^*) + \frac{U}{R} (b_1 - a + \omega) \right\} \quad (67)$$

\overline{P} is readily obtained from (58') .

V. OPTIMIZATION

1. Specification of the blade motion.

For engineering purposes it is sufficient to restrict the blade motion to that of pitching oscillations about the mid-chord. Hence we set $y = \beta_1(t)x$. The propeller motion is periodic and consequently we take $\beta_1(t)$ to be

$$\beta_1(t) = \text{Re} [m \exp j(\theta + n)] \quad (68)$$

where the real constants m, n specify the amplitude and phase of the pitching relative to the "mean position" and are the parameters at our discretion to effect an "optimal" blade motion. Note that the pitching period $2\pi/\Omega$ is the same as the trajectory period.

From (68) and the kinematic boundary condition on the blade we obtain

$$b_0(t) = 2V \text{Re}[\beta_1(t)]$$

$$b_1(t) = \text{Re}[\dot{\beta}_1(t)]$$

while all other b_n coefficients identically vanish. The thrust and energy expressions (64)-(67) simplify to

$$\bar{T} = \frac{\pi\rho}{4} \text{Re} \left\{ [2\Omega R(a - 2b_1) i] + [(a + b_0)a^* - b_0 \omega^*] \right\} \quad (64')$$

$$\bar{E} = \frac{\pi^2 \rho \Omega}{8} |b_0 + b_1 + \omega_1|^2 \left[1 + O\left(\frac{\Omega}{U} \log^2 \frac{U}{\Omega}\right) \right] \quad (65')$$

$$\bar{T} = \frac{\pi\rho}{4} \text{Re} \left\{ [2\Omega R(a - \Omega - 2b_1) i] + [2(a - \Omega)\Omega] \right\} \quad (66')$$

$$\bar{E} = \frac{\pi^2 \rho \Omega}{8} \left[|b_0 + b_1 + \omega_1|^2 + \frac{2U}{\pi} \text{Re}(b_0 + b_1 + \omega_1) \right] \left[1 + O\left(\frac{1}{R} \log^2 R\right) \right] \quad (67')$$

The first term in square brackets in (64') and (66') is the Y-force contribution. Notice that they are essentially identical in form. In (66') the X-force contribution (appearing in the second brackets) is due solely to the singular force whereas in (64'') both the suction force and the pressure component in the x-direction appear. Observe that if $|b_0 + b_1 + \omega_1|$ vanishes, then so does \bar{E} . Another notable feature of the equations (64') - (67') is that only the time harmonic components associated with $\beta_1(t)$ and $\omega(t)$ (i. e. b_0, b_1, ω_1) survive the averaging process. This fact enables us to interpret the blade motion as an "effective" heaving and pitching.

2. The effective harmonic blade motion.

We know that b_0 and b_1 depend directly on β_1 (the precise dependence issuing from the kinematic expression $h_t + V h_x$). Suppose we consider the harmonic part of $\omega(t)$ as having a similar origin. We seek the harmonic blade motion $y = h_1(x, t)$ which will generate the normal velocity $\omega_1(t) x$. Hence, $h_1(x, t)$ must be the particular solution of

$$\left(\frac{\partial}{\partial t} + V \frac{\partial}{\partial x} \right) h_1(x, t) = \omega_1(t)x$$

The particular solution we obtain is unique upon ruling out the solutions which satisfy the homogeneous equation. The total harmonic blade motion $h_0(x, t) = h(x, t) + h_1(x, t)$ becomes

$$h_0(x, t) = \text{Re} \left\{ \left[\frac{\xi_0}{2} + (\xi_1 + j \xi_2) x \right] e^{i\theta} \right\} \quad (69)$$

where ξ_0, ξ_1, ξ_2 are real constants given by

$$\xi_0 = \frac{2V \omega_1}{\Omega^2} = \begin{cases} 2R & \text{Case I} \\ -\frac{2U}{\Omega} & \text{Case II} \end{cases} \quad (70a)$$

$$\xi_1 = m \cos n \quad (70b)$$

$$\xi_2 = m \sin n - \frac{\omega_1}{\Omega} = \begin{cases} m \sin n - \epsilon & \text{Case I} \\ m \sin n + \delta & \text{Case II} \end{cases} \quad (70c)$$

Equation (69) is an interesting representation of the harmonic motion of the blade for it demonstrates that an effective heaving motion prevails with a constant amplitude of $\frac{1}{2} \xi_0$ together with an effective pitching about $x = 0$. The pitching amplitude $|\xi_1 + j \xi_2|$ is variable via m and n as is the pitching phase angle $\text{tg}^{-1}(\xi_2/\xi_1)$.

3. Non-trivial blade motion with vanishing \bar{E}, \bar{T} and \bar{P}

We now consider the quantity $(b_0 + b_1 + \omega_1)$ which has some importance in the optimization. It is convenient to express it in terms of ξ_0, ξ_1, ξ_2 , namely

$$b_0 + b_1 + \omega_1 = \Omega [(r \xi_1 - \xi_2) + i(r \xi_2 + \xi_0 + \xi_1)] \quad (71)$$

where

$$r \equiv \frac{2V}{\Omega} = \begin{cases} \frac{2U}{\Omega} & \text{Case I} \\ 2R & \text{Case II} \end{cases} \quad (72)$$

When $b_0 + b_1 + \omega_1 = 0$ then we term $\xi_1 = \hat{\xi}_1$, and $\xi_2 = \hat{\xi}_2$ critical values where

$$\hat{\xi}_1 = \frac{-\xi_0}{(1+r^2)} \cong \begin{cases} \frac{-\epsilon^2}{2R} & \text{(Case I)} \\ \delta & \text{(Case II)} \end{cases} \quad (73a)$$

$$\hat{\xi}_2 = \frac{-r \xi_0}{(1+r^2)} \cong \begin{cases} -\epsilon & \text{(Case I)} \\ \delta & \text{(Case II)} \end{cases} \quad (73b)$$

Define new quantities $\zeta_0, \zeta_1, \zeta_2$ by

$$\zeta_0 = \xi_0 / (1+r^2) \quad (74a)$$

$$\zeta_1 = \xi_1 - \hat{\xi}_1, \quad \zeta_2 = \xi_2 - \hat{\xi}_2 \quad (74b)$$

Since the effective heaving is fixed ζ_0 is a constant whereas ζ_1 (ζ_2) measures the departure of ξ_1 (ξ_2) from the critical value $\hat{\xi}_1$ ($\hat{\xi}_2$).

Substituting (74) into (71) yields

$$b_0 + b_1 + \omega_1 = \Omega [(r\zeta_1 - \zeta_2) + i(r\zeta_2 + \zeta_1)] \quad (71')$$

and note that with the change of variable ζ_0 does not appear. In fact (74) was designed to accomplish this feature. It is instructive to express (64') - (67') in terms of $\zeta = (\zeta_0, \zeta_1, \zeta_2)$

$$\bar{T} = \frac{\pi\rho}{4} \frac{\Omega^2 V}{U} (1+r^2) [\zeta_0 \zeta_1 + r\zeta_0 \zeta_2] [1 + O(\frac{1}{r} \log^2 r)] \quad (64'')$$

$$\bar{E} = \frac{\pi\rho}{4} \Omega^2 V (1+r^2) \left[\frac{\pi}{r} (\zeta_1^2 + \zeta_2^2) \right] [1 + O(\frac{1}{r} \log^2 r)] \quad (65'')$$

$$\bar{T} = \frac{-\pi\rho}{4} \frac{\Omega^2 V}{U} (1+r^2) [\zeta_0^2 + \zeta_0 \zeta_2] [1 + O(\frac{1}{r} \log^2 r)] \quad (66'')$$

$$\bar{E} = \frac{\pi\rho}{4} \Omega^2 V (1+r^2) \left[\frac{\pi}{r} (\zeta_1^2 + \zeta_2^2) + \frac{\zeta_0 \zeta_2}{r} - \zeta_0 \zeta_1 \right] \cdot [1 + O(\frac{1}{r} \log^2 r)] \quad (67'')$$

We see that when $\zeta_1 = \zeta_2 = 0$ (that is, e. g. $n = \frac{\pi}{2}$ and $m = \omega_1 / \Omega$) then the mean energy loss identically vanishes as does the average thrust (64"). The mean thrust for Case II (when $\zeta_1 = \zeta_2 = 0$) is seen to be negative since $\bar{T} \sim -\zeta_0^2$ which implies that energy is extracted from the fluid. However, since $\zeta_0 \ll 1$ we may essentially treat \bar{T} as a vanishingly small quantity. Thus when ξ_1, ξ_2 assume critical values ($\hat{\xi}_1, \hat{\xi}_2$) we observe that the mean energy loss, thrust and power all vanish corresponding to no vortex shedding at the trailing edge. The instantaneous values of \dot{E}, T, P are then due solely to virtual mass contributions. This property has been observed earlier by Wu [2].

4. The optimal problem.

The average useful work $U\bar{T}$, rate of energy loss \bar{E} and power input \bar{P} is conveniently expressed in coefficient form by dividing each quantity by $\frac{\pi\rho}{4} \Omega^2 V(1+r^2)l$. From (64")-(65") for Case I

$$C_E \cong \frac{\pi}{r} (\zeta_1^2 + \zeta_2^2) = \frac{\pi}{r} [m^2 + 2m\zeta_0(\cos n + r \sin n) - (1+r^2)\zeta_0^2] \quad (75)$$

$$C_T \cong (\zeta_0 \zeta_1 + r \zeta_0 \zeta_2) = m \zeta_0 (\cos n + r \sin n) \quad (76)$$

From (66)"-(67)" for Case II

$$C_E \cong \frac{\pi}{r} \left[(\zeta_1^2 + \zeta_2^2) + \frac{\zeta_0 \zeta_2}{r} - \zeta_0 \zeta_1 \right] = \frac{\pi}{r} \left[m^2 + rm \zeta_0 (\sin n - \frac{1}{r} \cos n) - (1+r^2)\zeta_0^2 \right] \quad (77)$$

$$C_T \cong -(\zeta_0 \zeta_2 r + \zeta_0^2) = -r m \zeta_0 \sin n \quad (78)$$

whereas the power input coefficient is obtained from the conservation of energy expression $C_P = C_E + C_T$.

From (76) we observe that the maximum C_T is approximately $(r \zeta_0 m)$ corresponding to $n \cong \pi/2$. This result indicates that a large m is desirable but not so large that the linearization requirement $m \ll 1$ is violated. C_T vanishes for n in the second quadrant near π and subsequently becomes negative for larger phase angles. Similar remarks apply to (78). The presence of the multiplicative factor π/r in (75), (77) renders the energy loss a small quantity for all phase angles provided $m \ll 1$ is not violated, which appears eminently reasonable.

The optimization problem is stated as follows. We seek the pitching motion within the class of functions (68) which will minimize the energy loss C_E under the side condition of specified useful work (or thrust), say,

$$C_T = C > 0$$

while holding U, Ω, R, l fixed.

We introduce a function C_1 and the Lagrange multiplier $\tilde{\lambda}$ by

$$C_1 = C_E + \tilde{\lambda} (C_T - C) \quad (79)$$

and perform the optimization procedure on C_1 . The three unknowns $m, n, \tilde{\lambda}$ can be obtained from the equations

$$\frac{\partial}{\partial m} C_1 = 0 \quad (80a)$$

$$\frac{\partial}{\partial n} C_1 = 0 \quad (80b)$$

$$C_T = C > 0 \quad (80c)$$

Equations (75), (76), (79), and (80) provide for Case I the following optimal values of m , n :

$$m = C/\epsilon \ll 1 \quad (C > \epsilon^2) \quad (81)$$

$$n = \left(\frac{\pi}{2} - \frac{\epsilon}{2R} \right) . \quad (82)$$

In (81) $C = \epsilon^2$ is incompatible with the singular situation pointed out in sections 1, 3 and consequently we avoid it by specifying $C > \epsilon^2$.

For $C \approx \frac{1}{3} \epsilon$ say, then $T_{\max} = O(U\Omega R) \gg 1$.

The minimum C_E for fixed C_T obtainable under the constrained optimization for this case is

$$\min C_E = \frac{\pi}{R} \left(\frac{C^2}{\epsilon^2} + 2C \right) . \quad (83)$$

Similarly equations (77), (78), (79), and (80) provide the following optimal values for Case II.

$$m \approx \frac{C}{\delta} \ll 1 \quad (C > \delta^2) \quad (84)$$

$$n \approx \pi/2 \quad (85)$$

$$\min C_E = \frac{\pi}{R} \left(\frac{C^2}{\delta^2} - C \right) > 0 \quad (C > \delta^2) \quad (86)$$

$$C_T = C \quad (87)$$

Again the thrust can be quite large since $T_{\max} = O(\Omega^2 R^2) \gg 1$.

The optimal results presented above for the two cases displays a remarkable resemblance. The reason for this is that the useful

work developed in both the high and low speed propulsion modes results primarily from the local lift force on the blade.

5. Development of thrust.

The optimal blade motion is given by $y = -x(m \sin \theta)$ from which it is possible to trace the blade attitude in time. See figures (6a, b).

The ratio of the steady X to Y force contributions in the thrust expression (64') (under optimal conditions) is $\frac{\pi m}{2R}$ while the corresponding ratio of terms of (66') is $\frac{-\log(2R/\gamma)}{R^2}$. These ratios, being both negative, imply that the steady X contribution is an inertial drag. The smallness of the ratios clearly indicates that the principle thrust contribution is derived from projecting the local lift force along the ξ -axis.

To leading order the optimal instantaneous Y force (from (54)) is

$$Y \approx 2\pi\rho V^2 m \sin \theta \quad (88)$$

and is positive for $0 < \theta < \pi$ and negative for $\pi < \theta < 2\pi$. The direction of this force is displayed in figures (6a and b) where it is observed to act in a thrust producing capacity.

6. Efficiency.

The hydromechanic efficiency is defined as the ratio of the average useful work to the average total power input

$$\eta = \frac{U\bar{T}}{\bar{P}} = \frac{1}{1 + \frac{\bar{E}}{U\bar{T}}} \quad (89)$$

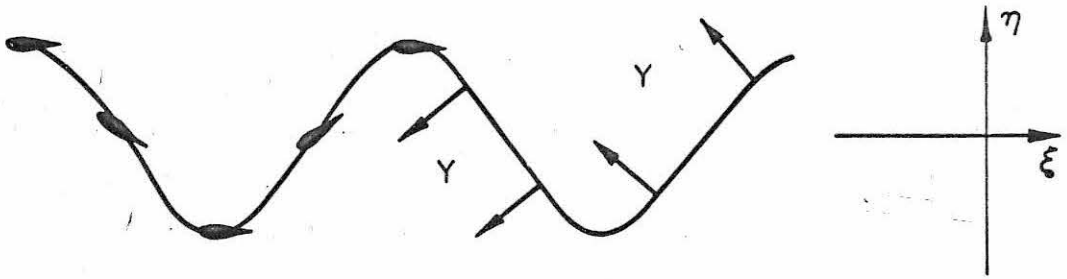


Fig. (6.a) Schematic representation of blade attitude and local lift force in the high speed propulsion mode.

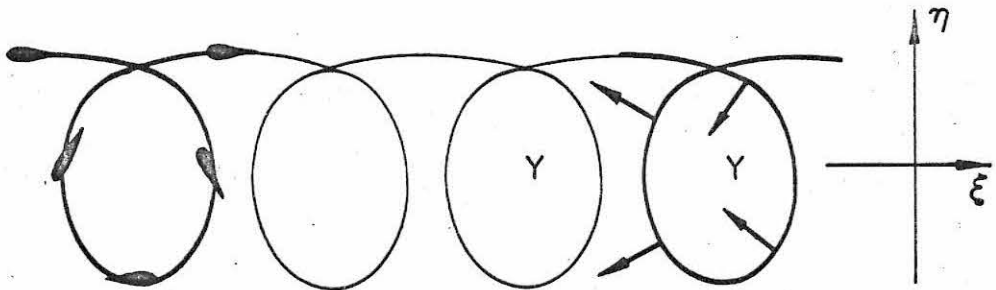


Fig. (6.b) Schematic representation of blade attitude and local lift force in the low speed propulsion mode.

We comment again that the energy loss always remains a small quantity because the amplitude of blade motion is restricted to small values. Hence the efficiency is largely governed by how we utilize the local lift force. Under optimum conditions the maximum efficiency is nearly unity for both Cases I and II. From equations (82), (83), (86), (87), and (89) we obtain:

$$\text{(Case I):} \quad \eta_{\max} \approx 1 - \frac{\pi}{2R} \left(\frac{C}{\epsilon} + 2\epsilon \right), \quad (\epsilon > C > \epsilon^2) \quad (90)$$

$$\text{Case II):} \quad \eta_{\max} \approx 1 - \frac{\pi}{2R} \left(\frac{C}{\delta^2} - 1 \right), \quad (\delta > C > \delta^2) \quad (91)$$

If we "push" the theory by permitting $C = \epsilon$ (equivalent to m finite) we see that η_{\max} for Case I is still near unity whereas $C = \delta$ for Case II gives $\eta_{\max} \approx \left(\frac{1}{1 + \frac{\pi\Omega}{2U}} \right)$. Here we observe a substantial loss in efficiency when Ω and U are of the same order. Consequently for Case II high efficiencies seem improbable for $C = \delta$ (unless $U \gg \Omega$).

7. Multiple Blades.

The performance features of a cycloidal propeller can be improved by increasing the number of blades. In figures (6a, b) we note that the instantaneous thrust force is greatly diminished at certain points of the flight path (e. g. at the peaks and troughs of figure (6a)) compared with its magnitude near the points where the ξ -axis intersects the trajectory. This situation leads to a surging motion and indicates that a single-bladed cycloidal propeller is unbalanced. A further manifestation of the imbalance of a single-bladed propeller is

the yawing motion which arises since the local lift force changes its direction during every half cycle of operation. The yawing motion can be substantially reduced by incorporating an additional blade 180° out of phase from the reference blade but such a blade arrangement would amplify the surging tendency. Clearly both surging and yawing motions can be considerably reduced by a four-bladed configuration each one 90° out of phase from the preceding blade.

VI. SUMMARY AND DISCUSSION

In this work we have developed a hydromechanical theory for cycloidal propellers. Two limiting cases of propeller operation have been considered, namely, the high speed propulsion mode of Case I wherein $U \gg \Omega R$ and the low speed propulsion mode where $\Omega R \gg U$. The high and low speed designations refer to the speed of advance of the propeller U , and do not necessarily imply that the blade speed V is greater in one case than in the other. It is assumed, however, that the characteristic Reynolds number based on the blade speed and the chord length is always large. This assumption excludes from consideration the case when the flight path is a common cycloid (or trajectories which are slight variations away from the common cycloid) since at certain stretches along such trajectories the blade speed can become very small indeed.

The investigation centers around the unsteady motions of a single thin blade which executes "small departures" from its "mean angular position". A blade occupies such a position when its chord is tangential to the flight path at its spanwise blade axis. The "small departures" we refer to may strictly be any blade motions wherein a linearized theory remains valid but specifically we consider only pitching motion about the mid-chord.

As we have mentioned earlier in the text, the quantitative results can be extrapolated to multi-bladed propellers provided the number of blades is limited to the extent that the mutual interference between the blades is not large. The interference nature of additional

blades may not always be adverse [15] and the investigation of this phenomenon using some of the ideas presented herein would provide a useful extension of this work. Such work would have particular relevance to the cycloidal propeller pursuing a prolate cycloidal flight path since there, each blade can operate in close proximity to a vortex sheet shed by another blade.

Three coordinate systems have been introduced in the study of this problem, namely, the fixed inertial system, the blade system (with its origin fixed to the central axis of the propeller), and the body system (with its origin fixed to the spanwise blade axis and with the x-axis tangential to the flight path). We use each of these systems at various stages of the development. The body system as we have defined it is particularly useful when dealing with hydromechanical problems involving small perturbations coupled with large amplitude motion.

Another formulation of the problem at hand might employ a coordinate system which has one axis fixed to the blade for all time. The analysis would be more complicated in such a frame of reference and when the blade executes only small perturbations its use is really not warranted. However, it is a natural vehicle for investigating larger departures from the "mean angular position" than are considered in this paper and there is much interest in this important problem. Clearly with such a coordinate system the situation involving the issuing of vorticity at the trailing-edge could be accounted for more accurately since it would then be unnecessary to neglect the small wavy motion of the approach which in fact is superposed on the

trajectory.

The hydrodynamical aspects of the problem commence with the momentum equation (Euler's equation) written in terms of the absolute velocity and pressure and with the variation of these dynamical quantities measured in the body frame of reference. This equation wherein fluid accelerations are balanced with pressure gradients is integrated along the mathematical characteristics to provide an explicit relationship for the complex absolute velocity $w(z, \tau)$ in terms of the complex acceleration potential $f(z, \tau)$. The result is derived and then simplified in Appendix I to yield a representation which is valid in the neighborhood of the blade, $z = O(1)$. The simplified form is used only to define the function of time, $A(\tau)$, of Eq. (29) which characterizes the time dependence of the leading-edge suction force. An approximation of a different nature is introduced to obtain an explicit relationship for $A(\tau)$, and the function $a(\tau)$, related to it through Eq. (38). This approximation concerns the replacement of the true characteristic by a curve which accurately represents it only over its initial stretch for distances of $O(1)$. Thereafter the two curves diverge. (We are essentially altering the path of integration in the integral equation for the determination of $a(\tau)$). However, the divergence of the curves occurs in a region where the effects of the past motion are small compared with the effects pertinent to the initial segment of the curve. Hence, the leading order term of $a(\tau)$ should be accurate. Physically this approximation appears to be reasonable since the prime influence on the

velocity at a point must be strongly dependent on those retarded pressures occurring in the immediate neighborhood of the point while those which are further removed in time and space must contribute in a diminished capacity. The idea is nicely demonstrated mathematically by von Karman and Sears [13]. In developing a higher order theory or particularly in those cases when the curvature of the trajectory is not so small, this approximation will not be adequate.

If the velocity field is desired it can be calculated (once the complex acceleration potential is known) from Eq. (9.A). The determination of the complex acceleration potential involves solving a straightforward Riemann-Hilbert boundary value problem.

Explicit expressions for the force and moment are obtained in Fourier coefficient form. These expressions become quite compact when the time averaging formula is applied to them, especially in the case when the blade motion is restricted to pitching only. In this latter form only the Fourier coefficients β_1 , b_0 , b_1 and the angular velocity term ω survive the averaging process.

Analytical expressions are developed for the total power input by considering the energy requirements necessary to sustain the propeller motion. Energy is supplied at the central axis in the form of a torque M_1 which imparts a rotational velocity to the blades. Additional energy is given to the blades at their spanwise pitching axis and this energy provides the power for the blades to pursue the flight path in the "mean angular position" and further, to execute the

small perturbations which are superposed on the "mean angular position". The torque at the central axis M_1 is of course related to the hydrodynamic forces produced by the motion of the blades. Using this information together with some geometrical identities enables us to write the total power input in the form of an energy balance equation $P = UT + \dot{E}$ and this equation expresses that in this inviscid model, part of the power input goes into producing useful work UT while the remainder represents a lost component which goes into maintaining the system of vortices in the wake.

In the optimal problem the energy loss is to be made as small as possible under the constraint of specified mean thrust, $C_T > 0$. Effective heaving and pitching motion variables are introduced into the thrust and energy coefficients and in terms of these variables a singular situation is easily recognized which corresponds to a non-trivial blade motion having zero mean power input, thrust and energy loss. This situation implies that the circulation about the blade remains constant and hence, non-zero instantaneous forces and moments are attributed to virtual mass contributions alone.

The solution to the optimal problem provides the pitching motion of the blade associated with the least energy loss while maintaining a specified mean thrust. The blade optimally operates at angles of attack where the local lift component lies inclined so as to always contribute to the useful work developed by the propeller.

The hydromechanical efficiency, defined as the ratio of useful work to total power input, can be impressively high for the

cycloidal propeller under optimum conditions. However, the high efficiencies found in the present theory are overly optimistic and lower values would be obtained in a theory which accounts for three dimensionality, blade interaction and the wake-crossing effect.

In Fig. 7 Mueller [14] displays some efficiency versus load coefficient curves which supply an indication of the potential of the cycloidal propeller as compared with a conventional screw propeller. The sinusoidal blade motion appears in an unfavorable light in this figure but apparently this is due to blade stalling, a situation which is avoided in the optimum blade setting.

We have mentioned earlier that the single bladed cycloidal propeller suffers an imbalance in the sense that surging and pitching motions are produced even though the blade delivers a specified mean thrust over one period of operation. The imbalance can be greatly reduced by a four-bladed configuration with each blade 90° out of phase from the preceding one but this is not to imply that a different blade configuration would have less merit.

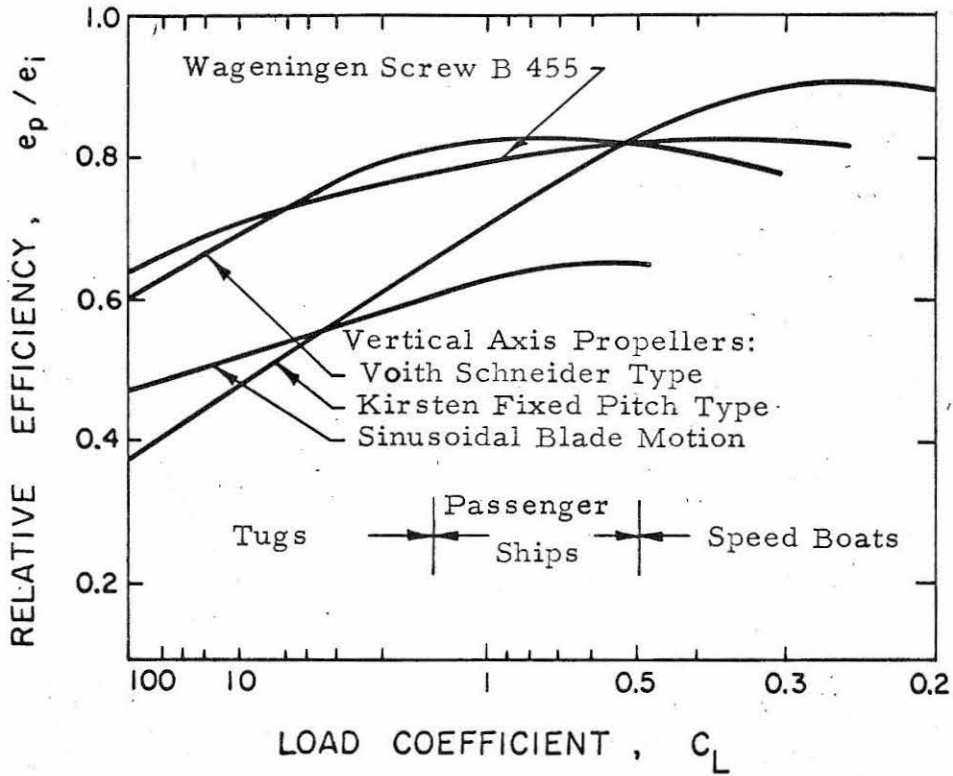


Fig. 7 Comparison between screw propellers and various types of vertical axis propellers.

$$C_L = \frac{\bar{T}}{2\rho U^2 A}$$

$$A = 2R \times (\text{span length})$$

$$e_p \equiv \eta = \frac{U\bar{T}}{P}$$

$$e_i = \frac{2}{1+(C_L+1)^{\frac{1}{2}}}$$

APPENDIX I

1. Integration of the Characteristic Equation

The Euler equation can be written as

$$B(z, \tau) \frac{\partial w}{\partial z} + \frac{\partial w}{\partial \tau} - i \kappa(\tau)w = \frac{\partial f}{\partial z} \quad (1. A)$$

where

$$B(z, \tau) = 1 - i \kappa(\tau)z \quad (2. A)$$

The mathematical characteristics of (1. A) are obtained upon integrating

$$\frac{dz}{d\tau} = B(z, \tau) \quad (3. A)$$

and this equation is amenable to integration when it is rewritten in the form

$$\frac{d}{d\tau} [ze^{i\nu(\tau;0)}] = e^{i\nu(\tau;0)} \quad (3. A')$$

where

$$\nu(\tau; \tau') = \nu(\tau; 0) - \nu(\tau'; 0) = \int_{\tau'}^{\tau} \kappa(\tau) d\tau \quad (4. A)$$

Performing the integration of (3. A') between the limits τ and τ' yields

$$z' = ze^{i\nu(\tau; \tau')} - \int_{\tau'}^{\tau} e^{i\nu(\tau; \tau')} d\tau \quad (5. A)$$

If we write the trajectory equation as a complex function $z = z_0(\tau'; \tau) = x_0(\tau'; \tau) + i y_0(\tau'; \tau)$ where (6) and (7) are expressed in terms of the variables τ, τ' , then

$$z_0(\tau'; \tau) = \int_{\tau'}^{\tau} e^{i\nu(\tau_1; \tau)} d\tau_1 \quad (6. A)$$

Substituting (6. A) into (5. A) yields the following convenient form for the characteristics,

$$z' = z'(\tau'; z, \tau) = e^{i\nu(\tau; \tau')} [z - z_0(\tau'; \tau)] \quad (7. A)$$

2. Integration of the Euler equation along the characteristics.

Along the characteristics (1. A) can be written as

$$\frac{dw}{d\tau} - i\kappa(\tau)w = \frac{\partial f}{\partial z} \quad (8. A)$$

and this equation possesses an integrating factor which enables us to rewrite it as

$$\frac{d}{d\tau} [we^{-i\nu(\tau; \tau')}] = \frac{e^{-i\nu(\tau; \tau')}}{B(z, \tau)} \left(\frac{df}{d\tau} - \frac{\partial f}{\partial \tau} \right) \quad (8. A')$$

Note that the operator identity $\left(\frac{d}{d\tau} - \frac{\partial}{\partial \tau} \right) = B \frac{\partial}{\partial z}$ has been used. If we integrate (8. A') along the characteristics from τ to τ' , we have (upon integrating the first term on the right hand side by parts and assuming zero initial conditions):

$$\begin{aligned} B(z, \tau)w(z, \tau) - f(z, \tau) &= i B(z, \tau) \int_{\tau}^{\tau'} \frac{f(z', \tau') \dot{\kappa}(\tau') z' e^{-i\nu(\tau'; \tau)}}{B^2(z', \tau')} d\tau' - \\ &- B(z, \tau) \int_{\tau}^{\tau'} \frac{\partial f}{\partial \tau'}(z', \tau') \frac{e^{-i\nu(\tau'; \tau)}}{B(z', \tau')} d\tau' \end{aligned} \quad (9. A)$$

where z' is given in (7. A). When f is known everywhere in the field of flow then (9. A) should be employed to give the corresponding velocity field. However, for purposes of calculating the instantaneous

forces on the blade we need not use the elaborate expression (9. A) which is valid everywhere. Instead, we use a simplified form which is uniformly valid when $z \approx O(1)$ (i. e. in the neighborhood of the blade). The desired form is most easily found by going back to the differential equation (1. A). Note that along a characteristic

$$\frac{d}{d\tau} (Bw) = B \left\{ \frac{dw}{d\tau} - i\kappa w \left[1 + \frac{\dot{\kappa} z}{\kappa(1-i\kappa z)} \right] \right\}. \quad (10. A)$$

For $z \approx O(1)$ then the term $\frac{\dot{\kappa} z}{\kappa(1-i\kappa z)} = O(\epsilon/R)$ for Case I ($\epsilon = \frac{\Omega R}{U} \ll 1$) and $O(\delta/R)$ for Case II ($\delta = \frac{U}{\Omega R} \ll 1$). In either case $\frac{\dot{\kappa} z}{\kappa(1-i\kappa z)}$ is negligible compared with unity and (1. A) when integrated along the characteristics gives

$$B(z, \tau)w(z, \tau) - f(z, \tau) = - \int_{\tau'}^{\tau} \frac{\partial f(z', \tau')}{\partial \tau'} d\tau' \quad (11. A)$$

REFERENCES

- [1] Wu, T. Y., "Hydromechanics of Swimming Propulsion. Part I. Swimming of a two-dimensional flexible plate at variable forward speeds in an inviscid fluid," Journal of Fluid Mechanics, 1971, Vol. 46, Part II.
- [1] Wu, T. Y., "Hydromechanics of Swimming Propulsion. Part II. Some Optimum Shape Problems," Journal of Fluid Mechanics, 1971, (to appear).
- [2] Wu, T. Y., "Swimming of a Waving Plate," Engineering Division, California Institute of Technology: Report No. 97-1.
- [3] Lighthill, M. J., "Aquatic Animal Propulsion of High Hydro-mechanical Efficiency," Journal of Fluid Mechanics, 1970, Vol. 44, Part II.
- [4] Haberman, W. and Hanley, E., DTMB Report 1564 (1961).
- [5] Tanaguchi, K., "Approximate Solution of the Voith-Schneider Propeller," Journal of Zosen Kiokai (1944), Vol. 74.
- [6] Sparenberg, J. A., "On the Efficiency of a Vertical Axis Propeller," Third Symposium on Naval Hydrodynamics, High Performance Ships; N. S. P. Wageningen (1960).
- [7] Sparenberg, J. A. and deGraaf, R., "On the Optimum One-bladed Cycloidal Ship Propeller," Journal of Engineering Mathematics, Vol. 3 (1969).
- [8] Nakonechny, B. V., "Experimental Performance of a Six-bladed Vertical Axis Propeller," DTMB Report No. 1446 (1961).

References (Cont'd)

- [9] Henry, C., "A Survey of Cycloidal Propulsion," Stevens Institute of Technology, Report No. 728.
- [10] Isay, W., "Zur Behandlung der Stromung durch einen Voith-Schneider Propeller mit Kleinem Fortschrittgrad," Ingenieur Archiv, 1955, Vol. 23
- [11] Muskhelishvili, N. I., "Singular Integral Equations, (1953). P. Noordhoff, Ltd., Groningen, Holland.
- [12] Erdelyi, et al., "Table of Integral Transforms," Vol. I. Bateman Manuscript Project, California Institute of Technology.
- [13] von Kármán, T. and Sears, W., Collected works of Theodore von Kármán. Vol. III (1933-1939). Airfoil theory for non-uniform motion.
- [14] Mueller, H. F., "Recent Development in the Design and Application of the Vertical Axis Propeller," a paper presented at the Spring Meeting, Philadelphia, Penn., May 19-20, 1955, of the Society of Naval Architects and Marine Engineers.
- [15] de Graaf, R., "On Optimum Fish Tail Propellers with Two Blades," Ph.D. Thesis, Univ. of Groningen (Holland) 1970.